

Triplet Pairing in Neutron Matter

V. V. Khodel, V. A. Khodel, and J. W. Clark

*McDonnell Center for the Space Sciences and Department of Physics,
Washington University, St. Louis, MO 63130-4899*

Abstract

The separation method developed earlier by us [Nucl. Phys. **A598** 390 (1996)] to calculate and analyze solutions of the BCS gap equation for 1S_0 pairing is extended and applied to 3P_2 - 3F_2 pairing in pure neutron matter. The pairing matrix elements are written as a separable part plus a remainder that vanishes when either momentum variable is on the Fermi surface. This decomposition effects a separation of the problem of determining the dependence of the gap components in a spin-angle representation on the magnitude of the momentum (described by a set of functions independent of magnetic quantum number) from the problem of determining the dependence of the gap on angle or magnetic projection. The former problem is solved through a set of nonsingular, quasilinear integral equations, providing inputs for solution of the latter problem through a coupled system of algebraic equations for a set of numerical coefficients. An incisive criterion is given for finding the upper critical density for closure of the triplet gap. The separation method and its development for triplet pairing exploit the existence of a small parameter, given by a gap-amplitude measure divided by the Fermi energy. The revised BCS equations admit analysis revealing universal properties of the full set of solutions for 3P_2 pairing in the absence of tensor coupling, referring especially to the energy degeneracy and energetic order of these solutions. The angle-average approximation introduced by Baldo et al. is illuminated in terms of the separation-transformed BCS problem and the small parameter expansion. Numerical calculations of 3P_2 pairing parameters and gap functions, with and without coupling to the 3F_2 state, are carried out for pairing matrix elements supplied by (vacuum) two-neutron interactions that fit nucleon-nucleon scattering data. It is emphasized that *ab initio* evaluation of the in-medium particle-particle interaction and associated single-particle energies will be required if a reliable quantitative description of nucleonic superfluids is to be achieved.

1 Introduction

The study of superfluidity in infinitely extended nuclear systems has a long history [1–82], predating the 1967 discovery of pulsars [83], which were soon

identified as rapidly rotating magnetic neutron stars [84]. Interest in nucleonic pairing has intensified in recent years, owing primarily to experimental developments on two different fronts. In the field of astrophysics, a series of X -ray satellites (including Einstein, EXOSAT, ROSAT, and ASCA) has brought a flow of data on thermal emission from neutron stars, comprising both upper limits and actual flux measurements. The recent launching of the Chandra X -ray observatory provides further impetus for more incisive theoretical investigations. Realistic *ab initio* prediction of the microscopic physics of nucleonic superfluid components in the interiors of neutron stars is crucial to a quantitative understanding of neutrino cooling mechanisms [85–95] that operate immediately after their birth in supernova events, as well as the magnetic properties, vortex structure, rotational dynamics, and pulse timing irregularities [96–99] of these superdense stellar objects. In particular, when nucleonic species enter a superfluid state in one or another region of the star, suppression factors of the form $\exp(-\Delta_F/k_B T)$ are introduced into the expression for the emissivity, Δ_F being an appropriate average measure of the energy gap at the Fermi surface. On the terrestrial front, the expanding capabilities of radioactive-beam and heavy-ion facilities have stimulated a concerted exploration of exotic nuclei and nuclei far from stability, with special focus on neutron-rich species [100,101]. Pairing plays a prominent role in modeling the structure and behavior of these new nuclei.

In this article we will be principally concerned with nucleonic pairing in the astrophysical setting. To a first approximation, a neutron star is described as a neutral system of nucleons (and possibly heavier baryons) and electrons (and possibly muons) in beta equilibrium at zero temperature, with a central density several times the saturation density ρ_0 of symmetrical nuclear matter [102,103,98,104,99]. The gross structure of the star (mass, radius, pressure and density profiles) is determined by the Tolman-Oppenheimer-Volkov general relativistic equation of hydrostatic equilibrium, consistently with the continuity equation and the equation of state (which embodies the microscopic physics of the system). The star contains (i) an *outer crust* made up of bare nuclei arranged in a lattice interpenetrated by relativistic electrons, (ii) an *inner crust* where a similar Coulomb lattice of neutron-rich nuclei is embedded in Fermi seas of relativistic electrons and neutrons, (iii) a *quantum fluid interior* of coexisting neutron, proton, and electron fluids, and finally (iv) a *core region* of uncertain constitution and phase (but possibly containing hyperons, a pion or kaon condensate and/or quark matter).

It is generally accepted [55,57] that the neutrons in the background fluid of the inner crust of a neutron star will pair-condense in the 1S_0 state. Qualitatively, this phenomenon can be understood as follows. At the relatively large average particle spacing at the “low” densities involved in this region ($\rho \sim \rho_0/10$), the delocalized neutrons experience mainly the attractive component the 1S_0 interaction. However, the pairing effect is quenched at higher densities, $\sim \rho_0$

and beyond, due to the strong short-range component of this interaction. By similar reasoning, one expects 1S_0 proton pairing to occur in the quantum fluid interior, in a density regime where the proton contaminant (necessary for charge balance and chemical equilibrium) reaches a partial density $\rho_p \sim \rho_0/10$.

The energy dependence of the nucleon-nucleon (NN) phase shifts in different partial waves offers some guidance in judging what nucleonic pair-condensed states are possible or likely in different regions of a neutron star. A rough correspondence between baryon density and NN bombardment energies can be established through the Fermi momenta assigned to the nucleonic components of neutron-star matter [57], which provide a crude measure of the maximum relative momenta attained in the nuclear medium. In (pure) neutron matter, only $T = 1$ partial waves are allowed by the Pauli principle. Moreover, one need only consider partial waves with $L \leq 4$ in the range of baryon density – optimistically, $\rho < (3 - 4)\rho_0$ – where a nucleonic model of neutron-star material is tenable. The 1S_0 phase shift is positive at low energy (indicating an attractive in-medium force) but turns negative (repulsive) at around 250 MeV lab energy. Thus, unless the in-medium pairing force is dramatically different from its vacuum counterpart, the situation already suggested above should prevail: S-wave pairs should form at low densities but should be inhibited from forming when the density approaches that of ordinary nuclear matter.

The next lowest $T = 1$ partial waves are the three triplet P waves 3P_J , with $J = 0, 1, 2$, which are actually coupled by the tensor force to the triplet F waves with the same total angular momentum J . Of these channels, the first two are not good candidates for pairing. In the 3P_0 state, the phase shift is only mildly attractive at low energy, turning repulsive at a lab energy of 200 MeV, while the 3P_1 phase shift is repulsive at all energies. On the other hand, the 3P_2 phase shift is negative at all energies, and indeed is the most attractive $T = 1$ phase shift at energies above about 160 MeV. This exceptional attractive strength in the 3P_2 state is due mainly to the spin-orbit interaction and in part to the coupling to 3F_2 wave via the tensor component of the NN force. A substantial pairing effect in the 3P_2 – 3F_2 channel may be expected at densities somewhat in excess of ρ_0 , again assuming that the relevant in-vacuum interaction is not greatly altered within the medium.

The remaining $T = 0$ partial waves with $L \leq 4$ are both singlets: 1D_2 and 1G_4 . However, the 1D_2 phase shift, though positive over the energy domain of interest, is clearly dominated by the 3P_2 phase shift, while the 1G_4 phase shift, again positive, is even less important.

Therefore, in the conventional picture of neutron-star matter (see, however, ref. [63]), singlet and triplet pairing are operationally equivalent to 1S_0 and 3P_2 – 3F_2 pairing, respectively. There have been many illuminating studies of the former problem, notably [41,55,48,67,78]. Here we shall concentrate on

triplet pairing in the pure neutron system, ignoring the relatively minor modifications that arise in beta-stable neutral matter with its dilute admixture of protons.

BCS theory [105,106] furnishes a general framework for microscopic treatments of nucleonic pairing. As is the case for singlet pairing [55,67], two rather different problems must be overcome to realize a quantitative description of triplet pairing within this framework and make realistic predictions for the associated energy gap. The first problem to be solved is the construction of an accurate in-medium (or “effective”) particle-particle interaction that provides the pairing force, together with a consistent mass operator that provides the single-particle input for the BCS equation. The second problem is to solve the BCS gap equation (actually a system of gap equations when one deals with $J \neq 0$), once the inputs for the pairing matrix and normal-state single-particle energies have been determined.

This first task places great demands on even the most advanced tools of many-body theory. For 1S_0 pairing, there exists a “first generation” of results on this facet of the problem, obtained by several different approaches (Landau Fermi-liquid theory [32], the method of correlated basis functions [41,55], the polarization-potential approach [47,56] and diagrammatic perturbation theory [66]). However, little progress has been made on this aspect of 3P_2 – 3F_2 pairing, and the issue of modifications of the associated input pairing interaction and single-particle energies due to short- and long-range correlations inside the nuclear medium remains open. We shall not attempt to address this issue here. Rather, we shall be concerned with the task of actually solving the triplet BCS system, assuming the particle-particle interaction is identical with the bare or vacuum NN interaction, and that the input single-particle energies needed to complete the BCS equation(s) have the same form as for free particles (perhaps with an effective mass). This problem also proves to be nontrivial, since we face essentially the same difficulties as in singlet S-wave pairing, and more:

- (a) Again, the kernel of the BCS gap equation(s) has a pole at zero gap amplitude, implying an incipient logarithmic divergence.
- (b) Again, the nonlocality of the particle-particle interaction in momentum space implies slow convergence of the integral over momentum modulus k in the BCS equation(s) – precluding application of the standard weak-coupling estimates of BCS theory [106]. This feature of nucleonic pairing implies that one must integrate out to large values of the momentum variable.
- (c) As already intimated, an additional complication of pairing in higher angular momentum states with $J \neq 0$ arises from the (possible) angle-dependence of the gap, which can be parametrized in terms of dependences on the quantum numbers J, L of the total and relative orbital

angular momenta and on the magnetic quantum number M associated with J . One must deal with a set of coupled gap equations for the gap components $\Delta_L^{JM}(k)$ in an expansion of the (generally anisotropic) gap in the spin-angle functions $\hat{G}_L^{JM}(\mathbf{n})$.

The combination of difficulties (a) and (b) can make numerical solution of the gap equation(s) a problematic exercise. To overcome these obstacles, a special procedure called the separation approach has been introduced in ref. [67] and applied to 1S_0 pairing. In this approach, the generic pairing matrix $V(k, k')$ is decomposed, identically, into a separable part, plus a remainder whose every element vanishes when either momentum variable lies on the Fermi surface. (As is characteristic of BCS theory, we assume that the particle-particle interaction is independent of frequency.) Applied to 1S_0 pairing, this separation procedure reduces the BCS gap equation to two equivalent coupled equations: a nonsingular, quasilinear integral equation for the shape of the gap function and a nonlinear equation determining its amplitude at the Fermi surface. We hasten to point out that this strategy is by no means limited to the case where the pairing matrix elements are supplied by the bare NN interaction – it will retain its practical and analytical value when a realistic in-medium particle-particle interaction is employed.

The primary aim of this article is to generalize the separation approach to pairing in an arbitrary angular momentum channel and apply it to 3P_2 pairing in neutron matter. Since, according to consideration (c) above, we are now confronted – in general – with a set of coupled gap equations rather than a single one, the situation is much more complicated than for 1S_0 pairing. However, in this case the power of the separation method becomes even more apparent. It enables a decomposition of the problem into (i) the determination of the shape of the gap function in k -space through an appropriate nonsingular quasilinear integral equation whose kernel is practically independent of the energy gap, and, once this is done, (ii) the determination of a set of numerical coefficients specifying the angular dependence of the gap through a system of nonlinear ‘algebraic’ equations.

In both singlet and triplet cases, the effectiveness of the separation scheme is greatly enhanced by the existence of a small parameter, given by the ratio of a suitable measure of the gap amplitude to the Fermi energy. Small-parameter expansions work well in the singlet problem, and even better in the triplet case. Corrections to the leading order in a small-parameter expansion of the 3P_2 – 3F_2 energy gap are down by a factor 10^{-5} or 10^{-6} . This property leads to considerable simplifications in the analytical and numerical treatment of the triplet problem, greatly ameliorating complication (c).

The separation approach is not merely a tool for numerical solution of gap equations. Following the lead of refs. [67,80,75,81], we shall demonstrate its

very important role in facilitating incisive analysis of the nature of pairing solutions in different angular momentum channels. In particular, the separation formalism provides a basis for establishing certain universal properties of 3P_2 pairing, properties that are independent of density and independent of the specifics of the pairing interaction itself, whether furnished by the in-vacuum or in-medium particle-particle interaction. The analytical results obtained here and in refs. [75,81] remain valid outside the context of neutron matter and carry implications for the still more complex problem of pairing in liquid ${}^3\text{He}$ [109].

In sect. 2, we display the BCS gap equations that describe pairing in an arbitrary two-body channel of given total spin S and isospin T . Sect. 3 extends the separation method of ref. [67] to this general problem, with special attention to 3P_2 - 3F_2 pairing. Sect. 4 is devoted to an analysis of 3P_2 pairing in the absence of tensor coupling to the 3F_2 state (“pure” 3P_2 pairing). We offer a straightforward criterion for determination of the upper critical density at which a solution of the pairing problem ceases to exist in the given two-body channel, in terms of vanishing of a characteristic determinant associated with the separation formulation. In sect. 5 we introduce the small-parameter expansion of the pairing problem and use it to clarify the nature of the angle-average approximation proposed by Baldo et al. [53]. In turn, the latter approximation is adopted to formulate an efficient procedure that allows reasonably accurate numerical solution of the coupled-channel, 3P_2 - 3F_2 pairing system when the goal is to find the magnitude of the pairing effect and the detailed structure of the pairing solutions is a lesser concern. We go on to recount how the fundamental character of the diverse solutions of the non-linear pairing problem may be elucidated within the separation method. The derivation of universal features of 3P_2 pairing is exemplified and discussed. Results from numerical application of the separation approach to triplet pairing in neutron matter are reported in sect. 6. Three representative models of the free-space NN interaction are used to construct pairing matrix elements, the Argonne v_{18} potential [107] being chosen as an example from the current generation of models yielding high-precision fits of the NN scattering data [108]. The results presented explicitly include the critical upper density for gap closure, the momentum dependence of gap components, and the conventional average measure of the gap amplitude at the Fermi surface, variously calculated for “pure” and tensor-coupled 3P_2 pairing, with and without use of the angle-average approximation. These results are compared with previous findings of other authors. In sect. 7, we indicate some promising future directions for research on pairing in infinitely extended nucleonic systems. An appendix reviews the separation method as developed for 1S_0 pairing. Small-parameter expansion is employed to devise an approximation for the gap amplitude that may be taken as a generalization of the BCS weak-coupling formula. Additionally, the technique of small-parameter expansion is extended to the triplet pairing problem.

2 Any-channel gap equation

To describe pairing in an arbitrary two-body state with total spin S , angular momentum J , and isospin T , it is useful to introduce a 2×2 gap matrix $\hat{\Delta}(\mathbf{k})$ which has the expansion (cf. [57,30])

$$\hat{\Delta}(\mathbf{k}) = \sum_{LJM} \Delta_L^{JM}(k) \hat{G}_L^{JM}(\mathbf{n}) \quad (1)$$

in the spin-angle matrices

$$\hat{G}_L^{JM}(\mathbf{n}) \equiv \sum_{M_S M_L} \langle \frac{1}{2} \frac{1}{2} \sigma_1 \sigma_2 | S M_S \rangle \langle S L M_S M_L | J M \rangle Y_{L M_L}(\mathbf{n}), \quad (2)$$

with $\mathbf{n} \equiv \mathbf{k}/k$. The total spin and isospin quantum numbers S, T ($= (1, 1)$ for triplet states and neutron matter) are fixed throughout and generally suppressed. Setting $S_{L'L_1}^{JM J_1 M_1}(\mathbf{n}) = \text{Tr} [\hat{G}_{L'}^{JM*}(\mathbf{n}) \hat{G}_{L_1}^{J_1 M_1}(\mathbf{n})]$, the spin-angle matrices (2) may be shown to obey the orthogonality condition

$$\int S_{L'L_1}^{JM J_1 M_1}(\mathbf{n}) d\mathbf{n} = \delta_{L'L_1} \delta_{J J_1} \delta_{M M_1}. \quad (3)$$

The particle-particle interaction has the corresponding expansion

$$V(\mathbf{k}, \mathbf{k}') = \sum_{LL'M} \langle k | V_{LL'}^J | k' \rangle \hat{G}_L^{JM}(\mathbf{n}) \hat{G}_{L'}^{JM*}(\mathbf{n}'), \quad (4)$$

with $|L - L'| \leq 2$ in the case of tensor forces. The coupled set of generalized gap equations for the components $\Delta_L^{JM}(k)$ then reads

$$\Delta_L^{JM}(k) = \sum_{L'L_1 J_1 M_1} (-1)^\Lambda \int \langle k | V_{L'L_1}^{L' J} | k' \rangle S_{L'L_1}^{JM J_1 M_1}(\mathbf{n}') \frac{\Delta_{L_1}^{J_1 M_1}(k')}{2E(\mathbf{k}')} d\mathbf{n}' d\tau', \quad (5)$$

with $\Lambda \equiv S + (L - L')/2$ and $d\tau' \equiv (2/\pi)(k')^2 dk'$. The energy denominator $E(\mathbf{k}) = [\xi^2(k) + D^2(\mathbf{k})]^{1/2}$ involves the square of the single-particle excitation energy $\xi(k) = \varepsilon(k) - \mu$ of the normal system, measured relative the Fermi energy μ , and a term

$$D^2(\mathbf{k}) = \frac{1}{2} \sum_{LJ M L_1 J_1 M_1} \Delta_L^{JM*}(k) \Delta_{L_1}^{J_1 M_1}(k) S_{L L_1}^{JM J_1 M_1}(\mathbf{n}) \quad (6)$$

giving rise to an energy gap in the single-particle excitation spectrum of the pair-condensed system. Examination of the the explicit formula for the angular

factor $S_{LL_1}^{JM J_1 M_1}(\mathbf{n})$ reveals that a summation over total momentum J_1 must be present in (5) and (6). (This fact is well known in the theory of superfluid ^3He [109]: the anisotropic ABM phase is built of states with total momentum $J = 1$ and 2.) The sum over orbital momenta L' on the l.h.s. of (5) appears only when tensor forces are present and is then restricted by $|L - L'| \leq 2$ and parity conservation. On the other hand, the sum over L_1 resulting from the angular dependence of the gap contains, in principle, an infinite number of terms.

We identify the energy gap as $|D(\mathbf{k})|$ and note that it is in general angle dependent and in general has nodes. It is convenient to define an angle-averaged gap function $\Delta(k)$ through the positive root of

$$\Delta^2(k) \equiv \overline{D^2}(k) = \frac{1}{4\pi} \int D^2(\mathbf{k}) d\mathbf{n} = \frac{1}{4\pi} \frac{1}{2} \sum_{LJM} |\Delta_L^{JM}(k)|^2. \quad (7)$$

(The last equality follows from the orthogonality property (3).) Analogously to the $^1\text{S}_0$ pairing problem, the quantity (7), evaluated at the Fermi momentum k_F and denoted $\Delta_F^2 \equiv \overline{D^2}(k_F)$ furnishes an overall measure of the strength of pairing correction to the ground-state energy in the preferred state. The notation $\overline{D^2}(k_F)$ is included here since it has been used earlier in the literature [57].

We take this opportunity to caution the reader that the literature is inconsistent and sometimes vague in the choice of energy gap measure. Care must be taken in interpreting statements about the magnitude of “the gap.” Moreover, the choice made in normalizing or defining the pairing matrix elements is not uniform. We have attempted to be precise, and for the most part we follow the conventions established by Takatsuka and Tamagaki [24,57].

3 Separation formulation of the triplet pairing problem

Generalizing the separation technique developed in ref. [67] for the $^1\text{S}_0$ problem, we again split the pairing matrix elements into a separable part and a remainder $W_{LL'}^J(k, k')$ that vanishes when either of the momentum variables k, k' lies on the Fermi surface. Thus

$$\langle k' | V_{LL'}^J | k \rangle \equiv V_{LL'}^J(k, k') = v_{LL'}^J \phi_{LL'}^J(k) \phi_{LL'}^J(k') + W_{LL'}^J(k, k'), \quad (8)$$

where $v_{LL'}^J \equiv V_{LL'}^J(k_F, k_F) \equiv \langle k_F | V_{LL'}^J | k_F \rangle$ and $\phi_{LL'}^J = \langle k_F | V_{LL'}^J | k_F \rangle / v_{LL'}^J$. Substitution of this identity into the generic-channel gap equation (5) yields

$$\begin{aligned}
\Delta_L^{JM}(k) &= \sum_{L'} (-1)^\Lambda \int W_{LL'}^J(k, k') \sum_{L_1 J_1 M_1} S_{L'L_1}^{JM J_1 M_1}(\mathbf{n}') \frac{\Delta_{L_1}^{J_1 M_1}(k')}{2\sqrt{\xi^2(k') + \delta^2}} d\mathbf{n}' d\tau' \\
&= \sum_{L'} D_{LL'}^{JM} \phi_{LL'}^J(k)
\end{aligned} \tag{9}$$

where the coefficients

$$D_{LL'}^{JM} = (-1)^\Lambda v_{LL'}^J \int \phi_{LL'}^J(k) \sum_{L_1 J_1 M_1} S_{L'L_1}^{JM J_1 M_1}(\mathbf{n}) \frac{\Delta_{L_1}^{J_1 M_1}(k)}{2\sqrt{\xi^2(k) + D^2(\mathbf{k})}} d\mathbf{n} d\tau \tag{10}$$

(with $d\tau \equiv (2/\pi)k^2 dk$) are just numbers.

As in ref. [67] (see also the appendix), we have introduced a typical scale δ in place of the gap in single-particle spectrum, in the term of (9) involving the portion $W_{LL'}^J(k, k')$ of the pairing matrix that vanishes on the Fermi surface. Such terms are quite insensitive to the choice of this scale, since the vanishing of $W_{LL'}^J(k, k')$ at $k' = k_F$ ensures that the integral over k' receives its overwhelming contributions some distance from the Fermi surface where $D^2(k')$ is negligible compared to $\xi^2(k')$. In the present context where the gap functions are angle-dependent, it is important to note that the δ quantity may be regarded as angle-independent. Numerical calculations show that the final result is practically independent of the choice of δ and we shall normally take it to be zero.

Employing the orthogonality condition (3), one finds that only diagonal terms (meaning $L_1 = L'$, $J_1 = J$, $M_1 = M$) contribute to the sum on the l.h.s. of eq. (9), which becomes

$$\Delta_L^{JM}(k) - \sum_{L'} (-1)^\Lambda \int W_{LL'}^J(k, k') \frac{\Delta_{L'}^{JM}(k')}{2|\xi(k')|} d\tau' = \sum_{L'} D_{LL'}^{JM} \phi_{LL'}^J(k). \tag{11}$$

Henceforth we shall frequently suppress the fixed index J . The functions $\phi_{LL_1}^J(k) \equiv \phi^{LL_1}(k)$ superposed on the r.h.s. of (11) do not depend on M . Accordingly, the gap components $\Delta_L^M(k) = \Delta_L^{JM}(k)$ can be constructed as linear combinations

$$\Delta_L^M(k) = \sum_{L_1 L_2} D_{L_1 L_2}^M \chi_L^{L_1 L_2}(k) \tag{12}$$

of M -independent functions $\chi_L^{L_1 L_2}(k) = \chi_L^{J L_1 L_2}(k)$ multiplied by coefficients $D_{L_1 L_2}^M$ determined by eq. (10). It is helpful to regard the quantities $\Delta_L^M(k)$ as forming a vector $\vec{\Delta}^M$ with components indexed by L , and similarly the

functions $\chi_{L_1 L_2}^L(k)$ as composing a vector $\vec{\chi}^{L_1 L_2}$. The equations

$$\chi_L^{L_1 L_2}(k) - \sum_{L'} (-1)^\Lambda \int W_{LL'}(k, k') \frac{\chi_{L'}^{L_1 L_2}(k')}{2|\xi(k')|} d\tau' = \delta_{LL_1} \phi^{L_1 L_2}(k) \quad (13)$$

for the shape factors $\chi_L^{L_1 L_2}(k)$ are readily obtained from eq. (11). From this result we see that $\chi_L^{L_1 L_2}(k_F) = \delta_{LL_1}$ for any L_2 , since the potentials $W_{LL'}(k, k')$ vanish for k on the Fermi surface while $\phi^{L_1 L_2}(k_F) = 1$ for any L_1, L_2 . It is important to observe that the equations (13) are free from any log singularities and form a coupled system of *linear* integral equations. We further remark that these equations can be solved *without regard* to the values of the coefficients $D_{LL'}^{JM} = D_{LL'}^M$ given by the set of equations (10) with $\Delta_{L_1}^{J_1 M_1}(k) = \Delta_{L_1}^{M_1}$ expanded as in (12).

It is also important to take note of an essential difference in the reformulated equations (11)–(13) as compared to the original gap equations (5). The sum over orbital angular momenta L_1 in (5) is in principle infinite, while in (11) only the states with $L' = L$ and $L' = L \pm 2$ can contribute, due to the conservation of the total angular momentum J and parity. Therefore the number of components of the vectors $\vec{\Delta}^M$ and $\vec{\chi}^{L_1 L_2}$ does not exceed 3, since $|L - L'| \leq 2$ and in eqs. (11)–(13) the total angular momentum J has a fixed value. We may infer that, in the case of a 3P_2 – 3F_2 mixture where $J = 2$, orbital angular momentum quantum numbers beyond 5 contribute only to the numerical factors $D_{L_1 L_2}^M$.

It is instructive to write out eqs. (11) and (13) in extended form for the 3P_2 – 3F_2 problem. Using a symbolic notation in terms of the operator $T = W/2[\xi^2 + \delta^2]^{1/2}$, the system (11) reads

$$\begin{aligned} \Delta_1^M + T_{11}\Delta_1^M + T_{13}\Delta_3^M &= D_{11}^M \phi^{11} + D_{13}^M \phi^{13}, \\ \Delta_3^M + T_{31}\Delta_1^M + T_{33}\Delta_3^M &= D_{31}^M \phi^{31} + D_{33}^M \phi^{33}. \end{aligned} \quad (14)$$

Suppose all the coefficients $D_{LL'}^M$ are zero except D_{11}^M ; then the solution $\vec{\Delta}^M$ of (14), a two-component vector, reduces to

$$\Delta_L^M(k) = D_{11}^M \chi_L^{11}(k) \quad (L = 1, 3), \quad (15)$$

where the components χ_1^{11} and χ_3^{11} of $\vec{\chi}_{11}$ obey the pair of equations

$$\begin{aligned} \chi_1^{11} + T_{11}\chi_1^{11} + T_{13}\chi_3^{11} &= \phi^{11}, \\ \chi_3^{11} + T_{31}\chi_1^{11} + T_{33}\chi_3^{11} &= 0. \end{aligned} \quad (16)$$

The vector $\vec{\chi}_{13}$ is given by a second pair of equations,

$$\begin{aligned}
\chi_1^{13} + T_{11}\chi_1^{13} + T_{13}\chi_3^{13} &= \phi^{13}, \\
\chi_3^{13} + T_{31}\chi_1^{13} + T_{33}\chi_3^{13} &= 0,
\end{aligned} \tag{17}$$

derived by supposing that D_{13}^M is present but all other $D_{LL'}^M$ are zero. The remaining two pairs of equations for the vector functions $\bar{\chi}^{31}$ and $\bar{\chi}^{33}$, namely

$$\begin{aligned}
\chi_1^{31} + T_{11}\chi_1^{31} + T_{13}\chi_3^{31} &= 0, \\
\chi_3^{31} + T_{31}\chi_1^{31} + T_{33}\chi_3^{31} &= \phi^{31},
\end{aligned} \tag{18}$$

and

$$\begin{aligned}
\chi_1^{33} + T_{11}\chi_1^{33} + T_{13}\chi_3^{33} &= 0, \\
\chi_3^{33} + T_{31}\chi_1^{33} + T_{33}\chi_3^{33} &= \phi^{33}
\end{aligned} \tag{19}$$

are constructed in the same fashion. The general solution of the 3P_2 - 3F_2 pairing problem is given by eq. (12) with the indices L_1 and L_2 taking on the values 1 or 3. It is worth noting that the same system of equations arises when one deals with S - D pairing in the deuteron channel, except that the indices L_1 and L_2 then take on the values 0 and 2.

Let us return now to the problem of pairing in an arbitrary two-body channel. Having learned that the shape factors $\chi_L^{L_1L_2}(k)$ in the representation (12) may be found by solving a set of nonsingular linear integral equations independently of the coefficients $D_{L_1L_2}^M$, we must next consider the determination of these coefficients, assuming knowledge of the χ functions. Substitution of (12) into (10) provides a set of nonlinear ‘algebraic’ equations to be solved for the desired set of numbers:

$$\begin{aligned}
D_{LL'}^{JM} &= (-1)^\Lambda v_{LL'}^J \int \phi^{LL'}(k) \sum_{L_1J_1M_1L_2L_3} S_{L'L_1}^{MJ_1M_1}(\mathbf{n}) D_{L_2L_3}^{J_1M_1} \\
&\quad \times \frac{\chi_{L_1}^{JL_2L_3}(k)}{2\sqrt{\xi^2(k) + D^2(\mathbf{k})}} d\mathbf{n}d\tau.
\end{aligned} \tag{20}$$

In the vicinity of the (upper) critical value ρ_c of the density ρ where the gap value Δ_F vanishes, the term $D^2(\mathbf{k})$ in the denominator of (20) can be omitted, and in this case we arrive at a system of *linear* equations for the coefficients $D_{LL'}^{JM}$. The determinant of the linearized system should vanish at $\rho = \rho_c$, since by definition there is no solution at that point. Thus we obtain a new condition for gap closure. For example, in the case of 3P_2 - 3F_2 pairing (where channel coupling is included), the zero of the determinant corresponding to the dominant $V_{11}^{J=2}$ matrix elements of the Argonne v_{18} potential [107] gives a value $k_c = 3.6 \text{ fm}^{-1}$ for the critical Fermi momentum when the input function

$\xi(k) = \varepsilon(k) - \mu$ in eqs. (20) is constructed from free single-particle energies $\varepsilon(k)$.

In the standard numerical approach to BCS pairing problems, the original system (5) for the gap components $\Delta_L^{JM}(k)$ is solved by iteration. One starts with suitable “guesses” for these functions (ten in number, for 3P_2 - 3F_2 pairing) and inserts them into the r.h.s. of (5), generating a new set of component functions; and so on until convergence is hopefully achieved. Such a procedure encounters obstacles even in the case of 1S_0 pairing [67,48,55]. A conventional iterative approach is even more problematic for pairing in higher angular momentum states, where the dimensionality of the nonlinear problem is much larger. From this point of view, Eqs. (20) are far more appropriate as basis for numerical computation, since shape factors $\chi_L^{L_1L_2}(k)$ are determined separately and iterations are needed only to find the set of coefficients $D_{L_1L_2}^{JM}$ entering the representation (12).

In principle, instead of trying to solve the system (20) directly, we could use the variables $D_{LL'}^{JM}$ (twenty in number, for 3P_2 - 3F_2 pairing) to parametrize the condensation energy and apply the variational principle to determine an appropriate set of these factors and a corresponding set of gap components $\Delta_L^{JM}(k)$. However, one must remember that the performance of optimization algorithms, as well as the convergence of iterative procedures, is very sensitive to the degeneracies of the functional under consideration. Accordingly, any attempt at implementing such an approach should be prefaced by a thorough study of the symmetries of the gap problem and the degeneracies of its solutions. Such a study is of considerable fundamental interest in any case [75].

4 Triplet-P pairing without channel coupling

To gain a better understanding of the triplet pairing problem in neutron matter, we revisit the pure (i.e., uncoupled) 3P_2 case analyzed in some detail in [24,57,40].

If tensor coupling to the 3F_2 state is neglected, the system of gap equations (5) reduces to a set of five equations, corresponding to $M = 0, \pm 1, \pm 2$. Taking into account the property of time-reversal invariance, which implies the relations

$$\left(\Delta_L^{JM}(k)\right)^* = (-1)^{J+M} \Delta_L^{J,-M}(k), \quad (21)$$

it is seen that only three of the generally complex components Δ_1^{2M} are independent. The independent components have customarily been written as

[24,57,40]

$$\begin{aligned}
\Delta_1^{20}(k) &= \delta_0(k), \\
\Delta_1^{21}(k) &= \left(\Delta_1^{2,-1}(k)\right)^* = \delta_1(k) + i\eta_1(k), \\
\Delta_1^{22}(k) &= \left(\Delta_1^{2,-2}(k)\right)^* = \delta_2(k) + i\eta_2(k),
\end{aligned} \tag{22}$$

where the $\delta_i(k)$ and $\eta_i(k)$ are real functions of k .

Takatsuka and Tamagaki [24,57], as well as Amundsen and Østgaard [40], have carried out numerical studies of the pure ${}^3\text{P}_2$ problem that demonstrate an interesting feature of triplet pairing in neutron matter (and in fact of triplet-P pairing more generally). Solutions of different types were found to be nearly degenerate, i.e., they yield very nearly the same condensation energy. The spread of condensation energies reported by Takatsuka and Tamagaki at a typical density is only 3%, and Østgaard and Amundsen obtained very similar results. The calculations of these authors were based on an older nucleon-nucleon potential called OPEG (see sec. 6 for details). Although this potential model is no longer competitive, its essential aspects are semi-quantitatively correct. At any rate, it will be argued that the nearly degenerate character of the level structure in the triplet pairing problem and the energy ordering of different solution types are very insensitive to the interaction assumed.

Important insights into the uncoupled problem can be achieved within the separation method [75]. For pure ${}^3\text{P}_2$ pairing, eq. (15) becomes simply

$$\Delta_1^{2M}(k) = D_{11}^{2M} \chi_1^{11}(k), \tag{23}$$

while the shape factor $\chi_1^{11}(k)$ obeys the uncoupled equation

$$\chi_1^{11}(k) + \int \frac{W_{11}(k, k') \chi_1^{11}(k')}{2|\xi(k)|} d\tau' = \phi^{11}(k). \tag{24}$$

We now make the decomposition $D_{112}^{M \neq 0} = (\lambda_M + i\kappa_M)\delta_0(k_F)/\sqrt{6}$, where $\delta_0(k_F) = D_{112}^{M=0}$ serves as a scale factor. Relations between the parameters λ_M and κ_M and the quantities $\delta_i(k_F)$ and $\eta_i(k_F)$ ($i = 1, 2$) stem from the definitions contained in eqs. (22). Evaluating the spin sums $S_{11}^{2M2M'}$ and separating real and imaginary parts in eq. (20), we extract the following set of equations determining the coefficients D_{11}^{JM} (cf. refs. [75,81]):

$$\begin{aligned}
\lambda_2 &= -v'[\lambda_2(J_0 + J_5) - \lambda_1 J_1 - \kappa_1 J_2 - J_3], \\
\kappa_2 &= -v'[\kappa_2(J_0 + J_5) - \kappa_1 J_1 + \lambda_1 J_2 + J_4], \\
\lambda_1 &= -v'[\lambda_1 J_6 - (\lambda_2 + 1)J_1 + \kappa_2 J_2 - \kappa_1 J_4/2],
\end{aligned}$$

$$\begin{aligned}
\kappa_1 &= -v'[\kappa_1 J_7 - \kappa_2 J_1 - (\lambda_2 - 1)J_2 - \lambda_1 J_4/2], \\
1 &= -v'[-(\lambda_1 J_1 - \kappa_1 J_2 + \lambda_2 J_3 - \kappa_2 J_4)/3 + J_5],
\end{aligned}
\tag{25}$$

where $v' = (\pi/2)v_{11}^{J=2}$. The integrals J_i are given by [75]

$$J_i = \int f_i(\theta, \varphi) \frac{\phi^{11}(k)\chi_1^{11}(k)}{2E(\mathbf{k})} k^2 dk \frac{d\mathbf{n}}{4\pi},
\tag{26}$$

with $f_0 = 1 - 3z^2$, $f_1 = 3xz/2$, $f_2 = 3yz/2$, $f_3 = 3(2x^2 + z^2 - 1)/2$, $f_4 = 3xy$, and $f_5 = (1 + 3z^2)/2$, where $x = \sin \theta \cos \varphi$, $y = \sin \theta \sin \varphi$, and $z = \cos \theta$. Of these integrals, only J_5 contains a principal term behaving like $\ln \Delta_F$, since only f_5 among the f_i does not vanish under the angular integration when multiplied by an angle-independent factor.

The normal-state single-particle energy $\xi(k)$ present in the energy denominator $E(\mathbf{k}) = [\xi^2(k) + D^2(\mathbf{k})]^{1/2}$ is conventionally assumed to have finite slope $d\xi(k)/dk$, while the gap term takes the explicit form

$$\begin{aligned}
D^2(\mathbf{k}) &= \frac{\delta_0^2}{16\pi} [(1 + \lambda_2)^2 + \kappa_1^2 + \kappa_2^2 + (\lambda_1^2 - 4\lambda_2 - \kappa_1^2)x^2 \\
&\quad - 2(\lambda_1 + \lambda_1\lambda_2 + \kappa_1\kappa_2)xz + (3 + \lambda_1^2 - \lambda_2^2 - 2\lambda_2)z^2 \\
&\quad + 2(2\kappa_2 - \kappa_1\lambda_1)xy + 2(\kappa_1 + \lambda_1\kappa_2 - \lambda_2\kappa_1)yz][\chi_1^{11}(k)]^2.
\end{aligned}
\tag{27}$$

In their angular content, the system (25) and the trigonometric decomposition (27) are consistent with the formulations of the uncoupled 3P_2 problem given in refs. [57,24,40], and specifically with eqs. (4.7)–(4.8) of Amundsen and Østgaard. However, our separation formulation, as expressed in eqs. (23)–(27), has distinct advantages as a basis for numerical solution of this problem. To begin with, there is only *one* shape function $\chi(k) \equiv \chi_1^{11}(k)$, which satisfies a linear integral equation of exactly the same form as for singlet-S pairing (cf. eq. (60)). This property of shape invariance follows naturally from the formal development presented in sect. 3. Given the key physical fact that the angle dependence of the problem only comes into play significantly in the close vicinity of the Fermi surface, we observe that this part of momentum space is almost entirely eliminated from the k' integration in eq. (24) by the vanishing of $W(k, k')$ at $k' = k_F$. Thus, to an excellent approximation, all solutions Δ_1^{2M} of the uncoupled triplet problem have identical shapes. In particular, the positions of their zeros and maxima coincide, as is clearly seen in the figures of previous works on triplet pairing in neutron matter [57,40].

To establish the angular dependences of the allowed solutions of the 3P_2 problem, the shape equation (24) must of course be supplemented by a set of equations that determine the coefficients or amplitudes corresponding to the

different M values. An important benefit of the separation strategy is that the nonlinear aspects of the problem are now concentrated entirely in the latter system of equations, given by (25) – equations for a set of *numbers* D_{112}^M rather than for a set of *functions*. By contrast, earlier authors [24,57,40] have worked directly with a set of singular linear integral equations for the five functions $\delta_0(k)$, $\delta_1(k)$, $\eta_1(k)$, $\delta_2(k)$, and $\eta_2(k)$ defined in eq. (22). In this approach, the dependences of gap quantities on the modulus of the momentum and on angles (or magnetic quantum numbers) are confronted simultaneously, with attendant opportunities for numerical difficulties.

Obviously, the process of numerical solution is facilitated by the separation of “shape” and “angular” aspects of the problem that has been accomplished in eqs. (23)–(27). Less obviously, this transformation opens the way to an incisive analysis of the nature of these solutions. Such an analysis has been carried out in refs. [75,81], extending the formalism to finite temperature T via introduction of the factor $\tanh[E(\mathbf{k})/k_B T]$ in the integrands of the basic gap equations eq. (5) and the J_i integrals (26).

Appealing to the orthogonality of the spherical functions for different M , it is possible to find special solutions of the system (25) (or of the system (4.7) of ref. [40]) that satisfy most or some of its equations identically. The simplest types of consistent solutions are characterized as follows [24,57,40]:

1. Only $M = \pm 2$ components are present: $\delta_0 = \delta_1 = \eta_1 = 0$.
2. Only $M = 0$ is present: $\delta_1 = \eta_1 = \delta_2 = \eta_2 = 0$.
3. Only $M = \pm 1$ are present: $\delta_0 = \delta_2 = \eta_2 = 0$.
4. Coupled case containing $M = 0, \pm 2$: $\delta_1 = \eta_1 = 0$.

In addition, there is naturally the general case involving all five M values.

For purposes of illustration, let us examine the situation for solution Types 1 and 2 in some detail.

Type 1. Under the assumption that only the component with $M = 2$ is present (its $M = -2$ partner being included trivially), we need only deal with $\Delta_1^{22}(k) = \delta_2(k_F)\chi(k)$, noting that a free choice of phase allows us to set $\eta_2 = 0$. In this case only the first of eqs. (25) is relevant and it becomes

$$\frac{1}{v} = - \int \phi(k)\chi(k) \frac{\frac{3}{2} \sin^2 \theta}{2\sqrt{\xi^2(k) + \frac{3}{2}\Delta_F^2 \chi^2(k) \sin^2 \theta}} d\mathbf{n}d\tau, \quad (28)$$

where $v = v_{11}^{J=2}$. All the other equations of the set (25) are met identically. (We remind the reader that Δ_F^2 is the value, on the Fermi surface, of the angle average defined in eq. (7).) Apart from the angular dependences and angular integration, eq. (28) has the same form as the equation (61) for the

gap amplitude in the 1S_0 problem (see the appendix). The angular integration can actually be performed analytically, with the result

$$\frac{1}{v} = - \int \frac{\phi(k)\chi(k)}{2\sqrt{\xi^2(k) + \frac{3}{2}\Delta_F^2\chi^2(k)}} \Phi_2(\beta_2) d\tau, \quad (29)$$

where

$$\begin{aligned} \Phi_2(\beta_2) &= \frac{3}{2\beta_2} \arcsin \beta_2 + \frac{3}{4\beta_2^2} \left[\sqrt{1 - \beta_2^2} - \frac{\arcsin \beta_2}{\beta_2} \right], \\ (\beta_2(k))^2 &= \frac{\frac{3}{2}\Delta_F^2\chi^2(k)}{\xi^2(k) + \frac{3}{2}\Delta_F^2\chi^2(k)}. \end{aligned} \quad (30)$$

The root of eq. (29) can be found numerically without difficulty, after finding the universal shape function $\chi(k) = \chi_1^{11}(k)$ by matrix inversion of the discretized form of eq. (24). This has been done for pairing matrix elements calculated from the OPEG potential employed by Takatsuka and Tamagaki [24,57] and Amundsen and Østgaard [40]; some results for this case are reported in sect. 6.

Type 2. Here there is the single component $\Delta_1^{20}(k) = \delta_0(k_F)\chi(k) = \Delta_F\chi(k)$. The dispersion equation determining Δ_F is given by the last of eqs. (25), which becomes

$$\frac{1}{v} = - \int \phi(k)\chi(k) \frac{\frac{1}{2}(1 + 3 \cos^2 \theta)}{2\sqrt{\xi^2(k) + \frac{1}{2}\Delta_F^2(1 + 3 \cos^2 \theta)\chi^2(k)}} d\mathbf{n} d\tau. \quad (31)$$

Analytic integration over angles is again possible, yielding

$$\frac{1}{v} = - \int \frac{\phi(k)\chi(k)}{2\sqrt{\xi^2(k) + \frac{1}{4}\Delta_F^2\chi^2(k)}} \Phi_0(\beta_0) d\tau, \quad (32)$$

where

$$\begin{aligned} \Phi_0(\beta_0) &= \frac{1}{2\beta_0} \ln \left(\beta_0 + \sqrt{1 + \beta_0^2} \right) + \frac{3}{4\beta_0^2} \left[\sqrt{1 + \beta_0^2} - \ln \left(\beta_0 + \frac{1}{\beta_0} \sqrt{1 + \beta_0^2} \right) \right], \\ (\beta_0(k))^2 &= \frac{\frac{3}{4}\Delta_F^2\chi^2(k)}{\xi^2(k) + \frac{1}{4}\Delta_F^2\chi^2(k)}. \end{aligned} \quad (33)$$

Some numerical results for this case are also reported in sect. 6, again for the OPEG potential.

5 Small-parameter expansion and angle-average approximation

Quantitative description of pairing in nuclear systems is beset with special difficulties because the strong inner repulsion (or strong momentum dependence) present in some partial waves (notably S states) implies that the momentum integral entering the gap equation must be extended to large momenta [48,55,67]. This behavior precludes the application of simple estimates such as the BCS weak-coupling formula, which assumes sharp localization of the pairing interaction around the Fermi surface. However, important simplifications are permitted by the existence of a small dimensionless parameter d_F , given essentially by the scale of the energy gap at the Fermi surface, relative to the value of the Fermi energy ε_F .

In the case of 1S_0 pairing, the small parameter is just $d_F = \Delta_F/\varepsilon_F$, where $\Delta_F \equiv \Delta(k_F)$. Framing this problem within the separation method, Taylor-series expansion of the energy denominator of the equation for the gap amplitude Δ_F has been employed in ref. [80] to derive a sequence of approximants for this quantity expressed as series of terms in $(d_F^2)^n \ln d_F$ and $(d_F^2)^n$ with integral n . The derivations involved are outlined in appendix A. Even the leading (zeroth) approximant yields reasonable results: the exact solution for Δ_F within the relevant density range is reproduced within 5%, based on pairing matrix elements formed from the 1S_0 component of the Argonne v_{18} interaction.

In the triplet case considered here, the small parameter is appropriately defined as $d_F = [\overline{D^2}(k_F)]^{1/2}/\varepsilon_F \equiv \Delta_F/\varepsilon_F$. A characteristic value of this quantity in the density region of interest is $0.5 \text{ MeV}/80 \text{ MeV} \simeq 6 \times 10^{-3}$, which is at least an order of magnitude smaller than typical values for singlet-S pairing. On this basis, one may expect to achieve good accuracy through an approximation that retains only the principal logarithmic terms $\sim \ln D^2(\mathbf{k})$ together with those independent of $D^2(\mathbf{k})$, while omitting corrections $\sim d_F^2 \ln d_F$. Small-parameter approximations are examined in more detail in the appendix. Here we restrict ourselves only to brief remarks.

Consider the integral on the r.h.s. of eqs. (20) for the coefficients $D_{LL'}^{JM}$. We may carry out an integration by parts with respect to the variable ξ , to derive a principal term (within the angular integration) that goes like $\ln D^2(k_F, \mathbf{n})$ and a remainder that involves $D^2(\mathbf{k})$ only in the factor

$$\ln \left(|\xi| + [\xi^2 + D^2(\mathbf{k})]^{1/2} \right).$$

Since latter quantity is quite smooth in the vicinity of the Fermi surface, its replacement by $\ln(2|\xi|)$ is valid within corrections of order of $d_F^2 \ln d_F$ that belong to the next stage of approximation. Writing $D^2(k_F, \mathbf{n}) = \Delta_F^2 \mathcal{D}^2(\mathbf{n})$, we extract the scale Δ_F^2 and express the angular dependence by $\mathcal{D}^2(\mathbf{n})$. The

dominant log term then decomposes as $\ln D^2(k_F, \mathbf{n}) = \ln \Delta_F^2 + \ln \mathcal{D}^2(\mathbf{n})$. By virtue of the orthogonality condition (3), the angle-independent portion $\ln \Delta_F^2$ contributes only to terms on the r.h.s. of eq. (20) that are diagonal in the magnetic quantum number, i.e., only for $M_1 = M$. Since Δ_F is a small quantity, the contribution from the scale term $\ln \Delta_F^2$ greatly exceeds that from the angle-dependent part $\ln \mathcal{D}^2(\mathbf{n})$, which remains of order of 1 even in the limit $\Delta_F \rightarrow 0$. It is worth noting that the Δ -independent contributions coming from terms in $\ln(2|\xi|)$ are also of order of 1. However, these terms are angle-independent and, like the scale term, contribute only to the diagonal part of the r.h.s. of (20). In fact, to within corrections of order $\sim d_F^2 \ln d_F$, the result for the D coefficients calculated from the angle-independent terms alone (i.e., dropping $\ln \mathcal{D}^2(\mathbf{n})$), is the *same* as the result we obtain if we simply replace the quantity $D^2(\mathbf{k})$ in the energy denominator of the original equation by its angle average (7),

$$\overline{D^2}(k) = \frac{1}{8\pi} \sum_L |\Delta_L^{JM=0}(k)|^2 + \frac{1}{4\pi} \sum_{LM>0} |\Delta_L^{JM}(k)|^2. \quad (34)$$

We reiterate that justification of this replacement, which corresponds to the *angle-average approximation* first introduced by Baldo et al. [53], rests on (i) the unimportance of the angle-dependent quantity $\ln \mathcal{D}^2(\mathbf{n})$ relative to $\ln \Delta_F^2$ and (ii) the unimportance of correction terms of order $d_F^2 \ln d_F$ or higher in the small parameter expansion. The angle-average approximation generally overestimates the pairing gap and the magnitude of the pairing energy (i.e. the pair condensation energy correction to the energy of the normal ground state). However, it allows a considerable simplification of the triplet pairing problem with very modest sacrifice in accuracy, if our primary interest lies in the magnitude of the pairing effect rather than the detailed structure of pairing solutions.

Making the replacement (34) in the general coupled-channel equations (20) for the gap amplitudes, we arrive at the quasi-uniform system

$$D_{LL'}^M = (-1)^\Lambda v_{LL'} \int \phi^{LL'}(k) \sum_{L_1 L_2} D_{L_1 L_2}^M \frac{\chi_{L_1 L_2}^{L_1 L_2}(k)}{2\sqrt{\xi^2(k) + \overline{D^2}(k)}} d\tau. \quad (35)$$

Since the index M appears explicitly only on the quantities being sought, there exists a degeneracy with respect to this quantum number: All sets of $D_{LL'}^{JM}$ yielding the same result for the gap quantity $\overline{D^2}(k)$ of eq. (34) are equivalent.

We first apply the angle-averaging prescription to the pure ${}^3\text{P}_2$ problem. In

this case eq. (35) becomes simply

$$1 = -v \int \frac{(\phi^{11}(k))^2 \chi_1^{11}(k)}{2\sqrt{\xi^2(k) + \overline{D}^2(k)}} d\tau \quad (36)$$

with $\overline{D}^2(k) = \Delta_F^2 [\chi_1^{11}(k)]^2 = \Delta_F^2 \chi^2(k)$ and $v = v_{11}^{J=2}$. This equation, having no explicit reference to magnetic substates, is identical in form to the singlet-channel equation (61) and is solved by the same method. Numerical results from solution of the uncoupled gap problem in this approximation are presented and discussed in sect. 6. If we do not care about the detailed angular behavior of solutions, but only about the size of the gap (as measured by Δ_F) and the condensation energy, the angular-averaging prescription gives very good predictions. This statement is justified by the close agreement with the results shown in fig. 1 for solution Types 1 and 2 and by the near degeneracy of the Δ_F values and condensation energies found numerically [24,57,40] and analytically [75] for the different solution types.

Turning to the general coupled-channel case, observe that the terms with $L_1 \neq L'$ on the r.h.s. of (35) contain integrals

$$A_{LL'}^{L_1 L_2} = \int \frac{\phi^{LL'}(k) \chi_{L'}^{L_1 L_2}(k)}{2\sqrt{\xi^2(k) + \overline{D}^2(k)}} d\tau \approx \int \frac{\phi^{LL'}(k) \chi_{L'}^{L_1 L_2}(k)}{2|\xi(k)|} d\tau \quad (37)$$

which are almost independent of the gap value, since the property $\chi_{L'}^{L_1 L_2} = \delta_{LL_1}$ implies that the numerators of the integrands vanish at the Fermi surface. In the diagonal case, $L_1 = L'$, we introduce an unknown positive number

$$Z = \int \frac{[\chi_1^{11}(k)]^2}{2\sqrt{\xi^2(k) + \overline{D}^2(k)}} d\tau \quad (38)$$

and write

$$\int \frac{\phi^{LL'}(k) \chi_{L'}^{L' L_2}(k)}{2\sqrt{\xi^2(k) + \overline{D}^2(k)}} d\tau \equiv Z + B_{LL'}^{L' L_2}, \quad (39)$$

where

$$B_{LL'}^{L' L_2} = \int \frac{\phi^{LL'}(k) \chi_{L'}^{L' L_2}(k) - [\chi_1^{11}(k)]^2}{2\sqrt{\xi^2(k) + \overline{D}^2(k)}} d\tau \approx \int \frac{\phi^{LL'}(k) \chi_{L'}^{L' L_2}(k) - [\chi_1^{11}(k)]^2}{2|\xi(k)|} d\tau. \quad (40)$$

The simplification on the right in eq. (40) is permitted since $\phi^{LL'}(k_F) = \chi_{L'}^{L' L_2}(k_F) = 1$ and the numerator in the integrands again vanishes at the

Fermi surface. The integrals $B_{LL'}^{L'L_2}$ are effectively already known: with the indicated simplifications, they only depend on the χ functions, which may be found from eqs. (13) without reference to the gap quantities $D_{LL'}^M$ being sought.

We now specialize to coupled-channel, 3P_2 - 3F_2 pairing where the system (35) for the coefficients $D_{LL'}^M$ contains four equations. For a solution of this set of equations to exist, the determinant

$$C(Z) = \begin{vmatrix} (1/v_{11}) + B_{11}^{11} + Z & B_{11}^{13} + Z & A_{11}^{31} & A_{11}^{33} \\ A_{13}^{11} & -(1/v_{13}) + A_{13}^{13} & B_{13}^{31} + Z & B_{13}^{33} + Z \\ B_{31}^{11} + Z & B_{31}^{13} + Z & -(1/v_{31}) + A_{31}^{31} & A_{31}^{33} \\ A_{33}^{11} & A_{33}^{13} & B_{33}^{31} + Z & (1/v_{33}) + B_{33}^{33} + Z \end{vmatrix}, \quad (41)$$

which depends on Δ_F (or the $D_{LL'}^M$ quantities) only through the parameter Z , must vanish. Evaluation of this determinant may be simplified by subtracting the third row from the second row and the second row from the fourth row, and then subtracting the second column from the first column and the third column from the fourth column. This leads to a *quadratic* equation for the determination of the unknown parameter Z :

$$C(Z) = c_2 Z^2 + c_1 Z + c_0 = 0, \quad (42)$$

where

$$c_0 = C(0) = \begin{vmatrix} C_{00} & C_{01} & C_{02} & C_{03} \\ C_{10} & C_{11} & C_{12} & C_{13} \\ C_{20} & C_{21} & C_{22} & C_{23} \\ C_{30} & C_{31} & C_{32} & C_{33} \end{vmatrix}, \quad (43)$$

$$c_2 = \begin{vmatrix} C_{30} - C_{10} - [C_{31} - C_{11}] & C_{33} - C_{13} - [C_{32} - C_{12}] \\ C_{00} - C_{20} - [C_{01} - C_{21}] & C_{03} - C_{23} - [C_{02} - C_{22}] \end{vmatrix}, \quad (44)$$

$$c_1 = C(1) - c_0 - c_2. \quad (45)$$

Equation (42) can have two roots $\{Z_0^\pm\}$, and only positive solutions are of interest.

Having found the appropriate root of (42), one may solve any three of the four equations of the system (35) for the ratios $D_{LL'}^M/D_{11}^M$. These ratios may

then be used to obtain an equation for D_{11}^M that is analogous to the algebraic equation for the gap amplitude Δ_F in the 1S_0 problem, namely

$$Z = \int \frac{[\chi_1^{11}(k)]^2}{2\sqrt{\xi^2(k) + \overline{D^2}(k)}} d\tau. \quad (46)$$

Solution of this equation yields the desired gap function in angle-average approximation.

The angle-average approximation serves well if the goal is to calculate the gap amplitude $\Delta_F = [\overline{D^2}(k_F)]^{1/2}$. However, if information is required on the spectrum of pairing solutions and the energy splittings between these solutions, it is essential to include the angle-dependent effects from the terms in eq. (20) going like $\ln \mathcal{D}^2(\mathbf{n})$. By so doing, accurate results and valuable insights can be gained even if we stop at leading order in the small-parameter approximation.

The situation is made more tangible by considering two simple solutions involving only one M value (and its negative), specifically $M = 2$ or $M = 0$ (corresponding to Types 1 and 2, respectively). Working at lowest order in the small-parameter expansion, partial integration of the definition (26) of the integrals J_i over the variable ξ leads to the simplified form

$$J_i = -\frac{1}{2} \int_0^1 \int_0^{2\pi} f_i(z, \varphi) \ln D^2(z, \varphi) \frac{dz d\varphi}{2\pi}, \quad (47)$$

having made use of the equalities $\phi(\xi = 0) = \chi(\xi = 0) = 1$. With this result, eqs. (28) and (31) are recast, respectively, as

$$1 = -vJ_5 \left(\Delta_F^{(M=2)} \right) \quad \text{and} \quad 1 = -v \left[J_0 \left(\Delta_F^{(M=0)} \right) + J_5 \left(\Delta_F^{(M=0)} \right) \right]. \quad (48)$$

The splitting between the states in question is determined by subtracting one equation from the other. Straightforward manipulations give

$$\ln \left(\frac{\Delta_F^{(2)}}{\Delta_F^{(0)}} \right)^2 = \frac{2}{3} - \ln 3 + \frac{2\pi}{9\sqrt{3}} \simeq -0.028. \quad (49)$$

When the angle-average approximation is applied, eq. (28) or (31) is replaced by

$$\frac{8\pi^2 \epsilon_F}{vk_F^3} + \int_1^\infty d\epsilon \frac{\sqrt{\epsilon+1}\phi\chi}{2\epsilon} + \int_{-1}^1 d\epsilon \frac{\sqrt{\epsilon+1}\phi\chi-1}{2|\epsilon|} + \ln \frac{4}{\Delta_F^2} - \ln \frac{1}{8\pi} = 0, \quad (50)$$

which is to be solved for $\Delta_F = \Delta_F^{\text{aa}}$. (Here, $\phi = \phi(\epsilon)$ and $\chi = \chi(\epsilon)$ after a change of integration variable from k to $\epsilon = (k/k_F)^2 - 1$.) Evaluating the ratios of $\Delta_F^{(2)}$ and $\Delta_F^{(1)}$ to Δ_F^{aa} along the lines of the above derivation of $\Delta_F^{(2)}/\Delta_F^{(0)}$, the ordering of the three gap amplitudes is seen to be $\Delta_F^{(2)} < \Delta_F^{(0)} < \Delta_F^{\text{aa}}$. This order agrees with the numerical results appearing in fig. 1 and with the findings of other authors [24,57,40].

It is interesting and highly significant that the result (49) for the ratio of pairing energies for the Type 1 ($|M| = 0$) and Type 2 ($M = 0$) solutions – obtained to leading order in the small parameter of the theory yet very accurate—is completely independent of the parameters of the actual interaction and independent of density. In other words, it is *universal*.

Proceeding to the next layer of complexity, let us consider the Type 4 solution, again studied in leading order. In this case, $M = 0$ and $|M| = 2$ substates coexist, and the system of equations that determines the coefficients D_{11}^{JM} becomes

$$\lambda_2 = -v [\lambda_2(J_0 + J_5) - J_3] , \quad (51)$$

$$1 = -v [-\lambda_2 J_3/3 + J_5] , \quad (52)$$

where we have introduced the more compact notation $\lambda_2 = \delta_2 \sqrt{6}/\delta_0$ and the J_i are given by (26). The first of these equations can be conveniently rewritten as

$$0 = \lambda_2 J_0 + (\lambda_2^2/3 - 1)J_3 \quad (53)$$

by subtracting λ_2 times eq. (52) from eq. (51).

The alternative form (53) is distinctly advantageous: unlike J_5 , the integrals J_0 and J_3 do not contain a term proportional to $\ln \Delta_F^2$ and hence are independent of any details of interaction. Consequently, eq. (53) provides a closed equation for the parameter λ_2 whose solution is universal – i.e., the same for all pairing interactions. Once the universal parameter λ_2 is determined, the scale parameter δ_0 is calculated from (52); its value does, of course, depend on the interaction.

The formulas for J_0 and J_3 can be further simplified by partial integration of J_0 over z and J_3 over φ . The remaining integration over φ is performed analytically. After simple operations, we arrive at

$$J_0(0, \lambda_2) = -\frac{1}{3} + 4 \int_0^1 \frac{z^2 dz}{f(z)} , \quad J_3(0, \lambda_2) = \frac{3 + \lambda_2^2}{4\lambda_2} - \frac{3}{8\lambda_2} \int_0^1 f(z) dz , \quad (54)$$

where $f(z) = [(1 + \lambda_2^2 + (3 - \lambda_2^2)z^2)^2 - 24\lambda_2^2(1 - z^2)^2]^{1/2}$. In general, these integrals are expressible in elliptic functions, but in exceptional cases they reduce to elementary integrals. This is exactly what happens when we seek roots of the system (51–53). In addition to the root $\lambda_2 = 0$ corresponding to the $M = 0$ state (the Type 2 solution), we find the roots $\lambda_2 = \pm 3$ and $\lambda_2 = \pm 1$. It should not be surprising that the roots are degenerate with respect to signs, since eq. (53) is invariant under reversal of the sign of λ_2 . What is most surprising is that these roots are rational numbers.

Rationality of the roots λ_2 is a consequence of a hidden symmetry of the problem that transcends the approximation we have employed. To substantiate this assertion, consider first the particular solution $\lambda_2 = 3$, for which the squared gap function (27) becomes $D^2(k, x, z; \lambda_2 = 3) \sim [\chi_1^{11}(k)]^2[4 - 3(x^2 + z^2)]$. The symmetry of this function with respect to x and z implies the relation $3J_0(0, 3) + 2J_3(0, 3) = 0$, since the combination $3f_0 + 2f_3 = 6(x^2 - z^2)$ changes sign on interchange of x and z whereas d^2 and other factors within the integrand of (26) are left unchanged. The above relation between J_0 and J_3 satisfies eq. (53). The essential point is that this relation derives from a simple symmetry of the problem; it is *not* predicated on any approximate scheme for the evaluation of the J_i . Now consider the root $\lambda_1 = 0$, for which $D^2(k, x, y, z) \sim [\chi_1^{11}(k)]^2(1 - x^2)$. Since $D^2(k, x, y, z)$ is independent of y and z , one may trivially integrate (26) over these variables. Simple algebra then gives $3J_0(0, 1) = 2J_3(0, 1)$, and this relation also satisfies Eq. (53). We may therefore conclude that the ratio of $M = 2$ and $M = 0$ components in the Type 4 solution is independent of any input parameters including density, temperature, and the parameters specifying the pairing interaction.

A general analysis along similar lines, again exploiting the simplifications produced by the separation method, reveals the fundamental structure of the full set of solutions of the BCS ${}^3\text{P}_2$ pairing problem in neutron matter [75]. Considering general multicomponent solutions, the allowed ratios of coefficients of different spin-angle matrices $\hat{G}_L^{JM}(\mathbf{n})$ in the expansion (1) of the gap matrix turn out to be universal. As in the above derivation, any reference to interaction, density, or temperature cancels out to very high accuracy in forming the ratios. The complete set of solutions for these ratios is obtained explicitly by solving a set of five coupled ‘algebraic’ equations, one of which serves to determine the energetic scale of the pairing effect. The solution set and the spectrum of pairing energies are found to be highly degenerate in character. The small splittings between different solutions can be found by manipulations similar to those performed above for the Type 1 and Type 2 solutions.

In principle, analogous analytic arguments may be used to establish universalities of pairing in the much more difficult problem of liquid ${}^3\text{He}$, where states with $L = S = 1$ and $J = 0, 1, 2$ contribute on an equal footing and the number of equations to be solved rises from five to nine.

6 Numerical applications: uncoupled and coupled channels

The separation approach to BCS-type pairing problems which has been further developed and studied in this paper leads to considerable simplifications of the process of solving the gap equations in a generic pairing channel. Aided by the existence of a small parameter, this approach allows one to find the *interval of existence* of solutions without having to perform any iterations, and it allows one actually to find *solutions* without having to iterate a set of integral equations. Some iterations may be required to construct solutions, but they need be performed only on a set of algebraic equations for the amplitudes of the components of the gap matrix (quantities that are momentum-independent but dependent on the magnetic projection M). The “division of labor” that underlies the separation method thus facilitates the process of finding solutions; moreover, because of the reduced number of numerical operations, it permits higher accuracy to be achieved. In addition to these numerical advantages, the new method offers an efficient framework for fundamental analytic investigations of pairing, as has been demonstrated in sect. 4 and more systematically in refs. [67,75,80,81].

A necessary step in testing our procedures for numerical solution of the triplet pairing problem in neutron matter is comparison with results obtained by other authors. As indicated in sect. 4, Takatsuka and Tamagaki [24] (see also their review [57]) have studied the pure 3P_2 pairing problem at some depth, classifying the types of solutions and generating numerical solutions by iteration. Subsequently, Takatsuka [30] (see also [57]) implemented an iterative procedure for solution of the gap equations in the 3P_2 - 3F_2 coupled-channel case with fixed $M = 0$. This early numerical work was based on several older potential models [110] with soft (Gaussian) cores. The Takatsuka-Tamagaki calculations were repeated and supplemented by Amundsen and Østgaard [40]. Baldo et al. [53] introduced the idea of angular averaging in considering $M = 0$ and $|M| = 2$ solutions (i.e., Type 2 and Type 1 solutions) of the pure 3P_2 case and reported preliminary numerical results for a separable approximation to the Argonne v_{14} potential [111]. More recently, Elgarøy et al. [69] have performed uncoupled 3P_2 and coupled 3P_2 - 3F_2 calculations with fixed $|M|$ (0 or 2) in β -stable matter for the Bonn potential models designated A, B, and C [112,113].

In the most recent microscopic study of triplet pairing, Baldo et al. [79] obtained results for several realistic models of the nucleon-nucleon interaction, including four that may legitimately be regarded as phase-shift equivalent. The latter potentials – Argonne v_{18} [107], CD-Bonn [114], and Nijmegen I and II [115] – belong to a new generation of models that yield high-precision fits of the sanitized world supply of pp and np scattering data up to a bombarding energy of 350 MeV. All four produce fits with χ^2 per data point close to

unity. In addition, gap calculations were performed for three “older” potentials – Argonne v_{14} , Paris [116], and Bonn B. The authors of this extensive study conclude that reliable predictions of the ${}^3\text{P}_2$ – ${}^3\text{F}_2$ pairing gap at densities above about 1.7 times the saturation density of symmetrical nuclear matter will require potential models that fit the nucleon-nucleon phase shifts up to 1 GeV.

For the purpose of comparison with the pre-1990 results on the triplet pairing problem, we have chosen the OPEG (“one-pion-exchange Gaussian”) potential [110] used in refs. [24,30,57,40], and specifically the version denoted OPEG ${}^3\text{O} - 1$. This potential has been fitted to scattering data collected before 1970, and it cannot be regarded as a realistic model of the nucleon-nucleon interaction. However, it possesses all of the essential qualitative features of the interaction and describes them at a semi-quantitative level. Of local character, it contains central, tensor, spin-orbit ($\mathbf{L} \cdot \mathbf{S}$), and quadratic spin-orbit (e.g. $(\mathbf{L} \cdot \mathbf{S})^2$) components, as written out in detail by Amundsen and Østgaard [40].

To compare with the latest calculations [79], we have generated results for the Argonne v_{14} and Argonne v_{18} models. The diagonal pairing matrix elements of these two potentials are plotted in fig. 2.

In presenting the numerical results, we employ two measures of the gap matrix, namely (i) the average quantity $\Delta_F \equiv [\overline{D^2}(k_F)]^{1/2}$ defined via eq. (7) or eq. (34) and (ii) the gap component $\Delta_L^{JM}(k)$, either as a function of the momentum modulus k or evaluated at the Fermi momentum k_F . We note that when the pairing problem is solved in the angle-average approximation specified in sect. 5, the M dependence of the latter measure becomes moot. Thus the index M will often be suppressed, along with the fixed index $J = 2$.

The zeros of the characteristic determinant of the linearized version of eq. (20) provide us with candidate values for the upper critical Fermi momentum k_c . This is true whether we restrict ourselves to pure ${}^3\text{P}_2$ pairing or address the coupled-channel ${}^3\text{P}_2$ – ${}^3\text{F}_2$ case. Examining first the uncoupled case, in fig. 3 we superimpose plots of the diagonal matrix elements $v_{11}^{J=2} = V_{11}^{J=2}(k_F, k_F)$ of the Argonne v_{18} potential, the associated characteristic determinant, and the gap component $\Delta_1^{2M}(k_F) = \Delta_1(k_F)$ obtained in the angle-average approximation, all considered as functions of the Fermi momentum k_F . From the preceding formal developments it is evident that a zero of the potential implies a pole of $\phi^{11}(k)$ and hence a simple pole of the determinant. Such a pole is very prominent in fig. 3 and is naturally followed closely by a zero of the determinant. The position of this zero gives a value $k_c \simeq 3.6 \text{ fm}^{-1}$ for the upper critical k_F value at which the gap closes, the corresponding upper critical density being $\rho_c = k_c^3/3\pi^2$. On the plot, the gap amplitude is clearly negligible at this point. Because of the exponential falloff, it appears to be zero even below this point,

but is in fact still finite over an interval in k_F where $v_{11}^{J=2}$ has positive values.

Fig. 4 displays the characteristic determinant in the coupled-channel case, again with the Argonne v_{18} potential as input for the pairing force. The determinant is evaluated for three different effective-mass ratios $m^* = M_n^*/M_n$, the free normal-state single-particle spectrum $\varepsilon(k) = \hbar^2 k^2 / 2M_n$ being replaced by $\hbar^2 k^2 / 2M_n^*$ to simulate dispersive effects of the medium. For any of the chosen values of m^* , the determinant has a pole near $k_F = 1.9 \text{ fm}^{-1}$ followed closely by a zero near $k_F = 2.2 \text{ fm}^{-1}$, and a second pole near $k_F = 3.3 \text{ fm}^{-1}$ followed closely by a zero near $k_F = 3.5 \text{ fm}^{-1}$. It is the second zero that should be identified with the upper critical density, since the adjacent pole corresponds to a zero of $v_{11}^{J=2}$. The point is that we are seeking to describe $T = 1$ triplet-P-wave pairing as modified by the tensor coupling to the $T = 1$ triplet-F channel. The first pole of the determinant corresponds to the zero of $v_{33}^{J=2}$. Thus the accompanying determinantal zero is not relevant to the task at hand, which is the identification of the upper critical point for triplet-P rather than triplet-F pairing. Generally, a *lower bound* on k_c for pairing predominantly in a state with orbital angular momentum quantum number L is given by the location of the pole that is produced by the vanishing of v_{LL}^J (we assume that this occurs only at one density). Conventional wisdom gives $v_{LL}^J < 0$ as a sufficient (but not necessary!) condition for a pairing instability in partial wave L . The indicated lower bound property is of course consistent with this statement, but we are able to provide a more incisive condition for the extent of the pairing instability in terms of the behavior of the characteristic determinant associated with the integral equation (20) (or alternatively, with the characteristic determinant of the integral equation (13) for the shape function $\chi(k)$ [80,117]). Concerning the dependence of k_c on effective mass, it is seen in fig. 4 that a smaller m^* leads to a lower value of the upper critical Fermi momentum (cf. further discussion below).

Numerical results for the OPEG interaction that may be compared with those of Takatsuka and Tamagaki and Amundsen and Østgaard (and with general findings of other authors) are displayed in fig. 1 and fig. 5. Fig. 1 refers to the uncoupled ${}^3\text{P}_2$ case with $m^* = 1$ and shows results for the k_F dependence of values of the energy-gap parameter Δ_F corresponding, respectively, to the angle-average approximation (uppermost curve), the pure $M = 0$ solution (middle curve), and the $|M| = 2$ solution (lowest curve). The latter two curves are in reasonable agreement with results reported in refs. [57,24,40], having maxima near 2 MeV in the vicinity of $k_F = 2.2 \text{ fm}^{-1}$. It is worth mentioning again that our calculations are in accord with the energy ordering of the $M = 0$ and $|M| = 2$ solutions found numerically in the early work [24,57,40]; moreover, they confirm the generic results that have been derived in sect. 5 using the separation method and the small parameter expansion. At $k_F = 2.2 \text{ fm}^{-1}$ the ratio predicted by eq. (49) is reproduced with better than 1% accuracy, and the energy order $\Delta_F^{(2)} < \Delta_F^{(0)} < \Delta_F^{\text{aa}}$ implied by eqs. (49) and (50)

is preserved. Considering the near-degeneracies in the condensation energies for the different solutions, documented originally by Takatsuka and Tamagaki [24], these favorable comparisons warrant some confidence in the application of the angle-average approximation to the coupled-channel case.

Introducing the coupling to the 3F_2 channel, we have solved the triplet pairing problem for the OPEG and Argonne potentials in the angle-average approximation, using the procedure outlined in sect. 5. Fig. 5 shows the calculated momentum dependence of the gap components $\Delta_1^{2M}(k) \equiv \Delta_1(k)$ (solid curve) and $\Delta_3^{2M}(k) \equiv \Delta_3(k)$ (dashed curve) for the case of the OPEG potential and $m^* = 1$, at a Fermi momentum $k_F = 2.2 \text{ fm}^{-1}$ near the value yielding the maximum strength of triplet pairing. The locations of the maxima, minima, and nodes of these functions are in close agreement with results given in refs. [30,57], and the magnitudes are in general agreement. (It is to be noted that in his coupled-channel calculation, Takatsuka included only the $M = 0$ magnetic substate.)

Figs. 6, 7, and 8 depict the principal results of our coupled-channel 3P_2 - 3F_2 gap calculations for the more realistic potential models, v_{18} and v_{14} . Fig. 6 illustrates the momentum dependence of the $L = 1$ and $L = 3$ components $\Delta_L^{2M}(k)$ for the Argonne v_{18} interaction (abbreviated as $\Delta_1(k)$ and $\Delta_2(k)$). As expected, the shapes of these gap functions are rather similar to those found for the OPEG interaction at the same density (cf. fig. 5). However, the overall scale of the pairing effect in the OPEG case is almost 50% larger than for the v_{18} model.

In fig. 7, we view the dependence of the gap component values $\Delta_2(k_F)$ and $\Delta_3(k_F)$ on the Fermi momentum k_F , as calculated in angle-average approximation for the v_{18} interaction. Contrasting the results for $\Delta_1(k_F)$ with and without coupling to the F wave, it is seen that the tensor force acts to substantially increase the pairing effect, as has been demonstrated in greater or lesser measure by earlier investigators [30,57,40,69].

Fig. 8 compares the k_F dependence of the 3P_2 - 3F_2 energy-gap parameter Δ_F for the three potentials investigated, the angle-average approximation being invoked in all cases. In all three cases, the gap measure Δ_F peaks in the range between $k_F = 2$ and 2.5 fm^{-1} . With the free single-particle spectrum, i.e., $m^* = 1$, the maximum value reached by this quantity for the v_{14} interaction is twice that attained for the more refined v_{18} model. As is clear from its definition, Δ_F contains direct contributions both from P-wave and F-wave pairing. Inspecting fig. 2, we observe that the greater pairing effect for the v_{14} potential relative to v_{18} can be traced to the greater attraction present for v_{14} in both P- and F-wave $J = 2$ channels over the relevant range of the momentum variable k . (The coupling matrix elements $V_{13}(kk)$ for the two potentials are essentially equivalent over the latter range.) Fig. 8 also

demonstrates the greater pairing effect of the OPEG potential relative to v_{18} . Such discrepancies between the predictions obtained for different interaction models are not unexpected: due to the log singularity intrinsic to the BCS pairing phenomenon, the overall strength Δ_F of the effect in the 3P_2 - 3F_2 channel is extremely sensitive to the behavior of the input pairing matrix elements at momenta in the vicinity of the Fermi surface. In turn, since the pairing matrix elements are constructed directly from the given free-space NN potential model and since $k_F \sim (2-3) \text{ fm}^{-1}$, one must expect a sensitive dependence on properties of the bare interaction that are not determined, or only poorly determined, by fits of the NN scattering data up to 350 MeV. This point has been developed thoroughly and convincingly in the recent work of Baldo et al. [79].

In table 1, we report some explicit numerical values of Δ_F obtained in our calculations based on the two “realistic” potential models, Argonne v_{14} and v_{18} . A comparison of our numerical results for these potentials with the corresponding results of Baldo et al. [79] is in order, restricting attention perforce to the case of free single-particle energies $\varepsilon(k)$. First, we point out that the pairing matrix elements entering our formulas are larger than those appearing in ref. [79] by a numerical factor $\pi/2$, due to different choices of normalization for the spherical Bessel functions. Upon accounting for this (immaterial) factor, the diagonal matrix elements plotted for the v_{18} interaction in fig. 3 of ref. [79] are apparently in excellent agreement with their counterparts in fig. 2. Second, it must be recognized that the quantity $D^2(k)$ defined in eq. (6) of ref. [79] is actually twice the function $D^2(k)$ appearing in our treatment (see our eqs. (6) and (34)). Thus the gap measure $\Delta_F \equiv [\overline{D^2}(k_F)]^{1/2}$ we have calculated is smaller than the Δ_F quantity of Baldo et al. by a factor $1/\sqrt{2}$. The definition we have adopted is motivated by the desideratum of consistency with the earlier literature [57,40]. In any case, the two calculations should agree once this scale factor is applied, since both calculations employ the angle-average approximation.

The results are generally in good agreement; however, there are some modest but significant numerical discrepancies. For the v_{14} interaction, the current results for Δ_F versus k_F are somewhat higher than those of ref. [79] below the peak, and somewhat lower above. The position of the peak, occurring near $k_F = 2.3 \text{ fm}^{-1}$ in the calculation of Baldo et al., is shifted to a slightly smaller k_F value, near 2.2 fm^{-1} . The value of Δ_F at the peak is higher in our calculation by roughly 5%. In the case of the v_{18} interaction, the numerical agreement is excellent below the peak, but beyond the maximum the current results lie below those of ref. [79] by an amount that can reach about 0.1 MeV (in the Δ_F measure used by Baldo et al.).

The origin of these relatively minor numerical disparities is not clear. We would, however, like to reiterate the concern expressed in refs. [69,79] about

the sensitivity of the numerical integration over k in the triplet gap equations to the choice of mesh points near the Fermi momentum. The difficulty arises because the functions $k^2\Delta_1^{2M}(k)/E(k)$ and $k^2\Delta_3^{2M}(k)/E(k)$ are very strongly peaked at k_F . To handle this problem within the present treatment, we have integrated out the troublesome log-like part by hand and performed a numerical integration only for the remainder, which is much smoother and well-behaved. For the latter integration, we employ 288 points, dividing the k domain into three intervals: $[0, k_F]$, $[k_F, 2k_F]$, and $[k_F, k_{\max}]$, with $k_{\max} = 50 \text{ fm}^{-1}$. Each interval contains 96 mesh points distributed in Gaussian fashion – very dense around the ends of the interval and sparse in the middle.

In fig. 8 and table 1, we have included v_{18} results not only for the baseline choice $m^* = 1$, but also for a value $m^* = 0.78$ of the effective-mass parameter conventionally thought [30,57] to provide a sensible representation of the in-medium single-particle energy. This brings us to the last point that we would like to address in the current treatment of triplet pairing in neutron matter. Relative to the bare-mass case, the propagator renormalization implied by $m^* = 0.78$ yields a substantially smaller gap as well as a lower value for the upper critical density (see fig. 4). These effects can be readily understood in terms of a reduction of the density of states $N(0)$ near the Fermi surface, which is related to the effective mass by the familiar expression $N(0) = k_F M_n^* / \pi^2 \hbar^2$. In the singlet-S-wave problem, the approximate formula (67) derived in the appendix shows clearly the inverse exponential dependence of the leading component of the gap on the density of states in the case of a negative pairing interaction on the Fermi surface, as does the BCS weak-coupling formula in a more limited context. The same physical reasoning and similar mathematical connections apply in the triplet case.

It is a common belief that at the higher densities where triplet pairing becomes important, the interactions with particles in the background neutron sea produce a considerably greater reduction from the bare mass than is the case at inner-crust densities where singlet pairing dominates [57,26]. This conclusion rests on the results of the Brueckner-Hartree-Fock and correlated-basis calculations. However, in these calculations, the contribution of pion-exchange effects to the renormalization of the nucleon effective mass is ignored. The role of the pion degrees of freedom grows rapidly with increasing density, eventually giving rise to a rearrangement of the ground state (associated, in particular, with pion condensation [118,119]). The latest variational prediction [120] of the density ρ_c at which this phase transition sets in is based on a nuclear Hamiltonian containing the Argonne v_{18} two-nucleon interaction (with boost corrections to account for the leading relativistic effects) and phenomenological three-nucleon interactions. The result $\rho_c \sim 0.2 \text{ fm}^{-3}$ actually lies below the density at which triplet pairing is expected to reach its maximum strength. Straightforward considerations [121,122] demonstrate that in the vicinity of this transition point the contribution of the pion-exchange diagram to the ef-

fective mass M_n^* diverges and m^* goes to infinity. Therefore it is not unlikely that the operative value of the effective mass in the domain of triplet pairing considerably exceeds the bare mass. From this standpoint, conventional treatments that assume an m^* value somewhat below unity may lose their relevance.

7 Prospectus

Exploiting the separation approach and the existence of a small parameter, we have been able to clarify important general properties of triplet pairing in neutron matter and to establish a framework and explicit procedures for reliable numerical solution of the relevant BCS gap equations. This effort complements a recent exhaustive analysis of the full set of generic solutions of the pure (uncoupled) 3P_2 problem, also performed with the aid of the separation strategy [75]. In view of the corresponding advances that have been made in the 1S_0 pairing problem [67,80,78], it can be reasonably claimed that the *mathematical and analytical* aspects of BCS pairing of identical fermions in 1S_0 and 3P_2 states are now well understood, both within the relevant nucleonic contexts and in a more universal, context-independent sense. The same cannot be said of the specific *physical and mechanistic* aspects of triplet or singlet pairing of strongly-interacting fermions, which are associated with the realistic in-medium particle-particle interaction and renormalized single-particle energies that should provide the raw material for the gap equations. A complete and realistic treatment of pairing in a given strongly-coupled Fermi system demands *ab initio* calculation of these essential inputs.

The success of the method of correlated-basis (or CBF) theory across a broad range of many-body systems and phenomena [124,55] suggests the following approach to the quantitative physics of pairing in extended nucleonic systems:

- (a) Dressing of the pairing interaction by Jastrow correlations within CBF theory [34,35]
- (b) Dressing of the pairing interaction by dynamical collective effects within CBF theory [35,41] (including polarization effects arising from exchange of density and spin-density fluctuations, etc.)
- (c) Consistent renormalization of single-particle energies by short- and long-range correlations within CBF theory (cf. ref. [123])

This approach has already been explored in the 1S_0 neutron pairing problem [41,55], although the assumed Jastrow correlations have not been optimized and only a second-order CBF perturbation treatment is available for step (b). Application of this scheme to 3P_2 - 3F_2 pairing in neutron-star matter is a challenging but potentially rewarding prospect.

The inclusion of other physical effects will also be important in achieving a realistic description of pairing in the neutron-star medium. Modifications due to three-nucleon interactions should be considered, the calculations should be performed in β -stable matter (cf. ref. [69]), and relativistic effects should be examined (see, for example, ref. [70,77]). As pointed out in sect. 6, the impact on pairing of mesonic degrees of freedom, especially through an enhancement of the nucleon effective mass in the vicinity of pion condensation, deserves close investigation.

In conclusion, it is important to emphasize that although the specific calculations performed in the present work were based on pairing matrix elements computed directly from bare, in-vacuum NN interactions and on quadratic single-particle energies, many of our findings are unaffected by these simplifications. Indeed, the analyses that have been performed (leading to the universal properties discussed here and in ref. [75]), as well as the calculational procedures that have been developed, will retain their applicability and essential validity when realistic in-medium inputs are employed in the gap equations.

Within this in mind, further studies in the same spirit – aimed at developing accurate computational procedures and uncovering universal properties – are of considerable interest. As a continuation of the work of sect. 6, the separation-transformed BCS gap equations for pure neutron matter may be solved in the 3P_2 – 3F_2 coupled channel without resorting to the angle-average approximation, but still within the setting of the rapidly convergent small-parameter expansion, and with bare pairing matrix elements and unrenormalized single-particle energies. Another project that awaits conclusion is a perturbative treatment of the lifting of the universalities and degeneracies that were established for the uncoupled 3P_2 pairing by the analysis carried out in ref. [75]. Also, the separation analysis performed in that paper may be extended to explore the superfluid phase diagram of liquid ${}^3\text{He}$ – although this task is considerably more demanding than in the case of 3P_2 pairing in neutron matter. Finally, application of the separation approach to studies of 3S_1 – 3D_1 pairing in symmetrical nuclear matter and in the expanding phase of heavy-ion collisions may produce new insights into these intriguing problems.

8 Acknowledgements

This research was supported in part by the US National Science Foundation under Grant Nos. PHY-9602127 and PHY-9900713 and by the McDonnell Center for the Space Sciences. We thank M. Hjorth-Jensen, Ø. Elgarøy, and R. B. Wiringa for stimulating discussions and helpful communications.

9 Appendix

In this appendix we review the application of the separation method to $^1\text{S}_0$ pairing [67] and display the first two approximants to the gap amplitude $\Delta_F \equiv \Delta(k_F)$ within a small-parameter expansion of the separated problem [80]. Having set the pattern, we then sketch the extension of the small-parameter expansion to $^3\text{P}_2$ pairing.

To provide a baseline for the separation method, it is useful to revisit the problem of a separable pairing matrix $V(k, k') = v_0 \phi(k) \phi(k')$ with $\phi(k_F) = 1$ and $v_0 \equiv V^{J=0}(k_F, k_F) \neq 0$. The standard gap equation in the $^1\text{S}_0$ channel,

$$\Delta(k) = - \int \frac{V(k, k') \Delta(k')}{2\sqrt{\xi^2(k') + \Delta^2(k')}} d\tau_0 \quad (55)$$

with $d\tau_0 = k^2 dk / 2\pi^2$, becomes

$$\Delta(k) = -v_0 \phi(k) \int \frac{\phi(k') \Delta(k')}{2\sqrt{\xi^2(k') + \Delta^2(k')}} d\tau_0. \quad (56)$$

(One may note that the differential volume element $d\tau_0$ entering eqs. (55)–(56) and other formulas below differs from the volume element $d\tau = (2/\pi)k^2 dk$ occurring in integrals elsewhere in this paper. The difference arises from a different choice of normalization in forming the pairing matrix elements. In this appendix, the S-wave pairing matrix elements are defined as in refs. [67,80], whereas the convention employed by Takatsuka and Tamagaki [57] for general pairing matrix elements is adopted in the rest of the paper.)

Since the integral on the r.h.s. of eq. (56) is just a number, we see that $\phi(k)$ determines the shape of the gap function, while the integral determines its scale. Introducing a dimensionless shape function $\chi(k)$ such that $\Delta(k) \equiv \Delta_F \chi(k)$, the gap equation for this problem is equivalent to

$$\chi(k) = \phi(k), \quad (57)$$

$$1 = -v_0 \int \frac{\phi^2(k)}{2\sqrt{\xi^2(k) + \Delta_F^2 \phi^2(k)}} d\tau_0. \quad (58)$$

Thus, one has only to solve a nonlinear equation for the gap amplitude rather than a nonlinear singular integral equation for the gap function. We note that a solution of this equation exists only when v_F is negative, in which case the monotonicity of the r.h.s. implies that there exists one and only one solution.

Now we turn to the general situation where $V(k, k')$ need not be separable. To gain some benefits of the separable case, let us split the pairing interaction into a separable part and a remainder that vanishes when either momentum variable is on the Fermi surface:

$$V(k, k') = v_0\phi(k)\phi(k') + W(k, k'), \quad (59)$$

where $W(k_F, k) = W(k, k_F) \equiv 0$ and, as before, $\phi(k) = V(k, k_F)/v_F$. Again writing $\Delta(k) = \Delta_F\chi(k)$, the gap equation (55) is readily seen to be equivalent to the integral equation for the shape function $\chi(k)$

$$\chi(k) + \int \frac{W(k, k')\chi(k')}{2\sqrt{\xi^2(k) + \Delta_F^2\chi^2(k)}}d\tau_0 = \phi(k), \quad (60)$$

together with the ‘algebraic’ equation

$$1 + v_0 \int \frac{\phi(k)\chi(k)}{2\sqrt{\xi^2(k) + \Delta_F^2\chi^2(k)}}d\tau_0 = 0 \quad (61)$$

for the gap amplitude Δ_F (assumed nonzero). It is important to note that since $W(k, k_F)$ is zero by construction, the integral equation (60) has a nonsingular kernel, the log-singularity of the original BCS formulation having been isolated in the amplitude equation (61). An iterative solution of this set of equations converges very rapidly. Indeed, for neutron matter at densities corresponding to the inner-crust region of a neutron star, a good approximation to the gap is already obtained by replacing $\Delta_F\chi(k)$ in the denominator of (60) by a small constant scale factor δ (e.g. $0.01\varepsilon_F$) solving (60) for $\chi(k)$ by matrix inversion, and substituting the result into (61) to obtain the scale factor Δ_F by (say) Newton’s method.

The existence of a small parameter $d_F = \Delta_F/\varepsilon_F$ for the problem plays a key role in the success of the separation method based on eqs. (60)–(61). Consider the equation (60) for the shape function $\chi(k)$. Since the Taylor expansion of the remainder function $W(k, k')$ around $k' = k_F$ starts with the first-order term $dW(k, k')/dk'|_{k'=k_F}(k' - k_F)$, the integral over k' in the symmetric vicinity $[k_F - \delta k, k_F + \delta k]$ of this point vanishes for sufficiently smooth functions $W(k, k')$ and $\chi(k)$,

$$\left. \frac{\partial^2 W(k, k')}{\partial k'^2} \right|_{k_F} \delta k \ll \left. \frac{\partial W(k, k')}{\partial k'} \right|_{k_F} \quad \text{and} \quad \frac{d\chi(k)}{dk} \delta k \ll 1. \quad (62)$$

Also, if beyond this interval we have $\Delta_F\chi(k) \ll \xi(k)$, or in other words if $\delta k \gg d_F k_F$, it is a safe approximation to replace the Δ_F term in the denominator

of (60) by a rather arbitrary scale factor δ . We thereby obtain a practically equivalent *linear* integral equation

$$\chi(k) + \int \frac{W(k, k')\chi(k')}{2\sqrt{\xi^2(k') + \delta^2}} d\tau_0 = \phi(k), \quad (63)$$

which is always soluble for well-behaved interactions. For most purposes, it is permissible simply to set δ equal to zero. The nature of this “ δ approximation,” and more generally of expansions in the small parameter d_F , is developed more fully below.

For realistic nuclear potentials, the accuracy of this approximation in the singlet-S problem is in fact *much* higher than indicated by the simple error estimate $d_F^2 \ln 1/d_F$ that accompanies the above preceding. The reason for this heightened accuracy is that the main contribution to the integral in (60) comes from a region well separated from the Fermi surface. The 1S_0 pairing matrix elements of realistic nuclear potentials show maxima at $k \sim 3 \text{ fm}^{-1}$. Hence the contribution from the Fermi surface region, already small because of the structure of $W(k, k')$, becomes quite negligible in comparison.

Based on Taylor-series expansion of the energy denominator of eq. (61), the gap amplitude Δ_F may be systematically expressed as a combination of series of terms in $(d_F^2)^n \ln 1/d_F$ and $(d_F^2)^n$ with integral n . Introducing the dimensionless variable $\epsilon(k/k_F)^2 - 1$, eq. (61) is first recast as

$$\frac{2}{N(0)v_F} + \int_{-1}^1 \frac{\sqrt{\epsilon+1}\phi(\epsilon)\chi(\epsilon)d\epsilon}{2\sqrt{\epsilon^2 + d_F^2\chi^2(\epsilon)}} + \int_1^\infty \frac{\sqrt{\epsilon+1}\phi(\epsilon)\chi(\epsilon)}{2\sqrt{\epsilon^2 + d_F^2\chi^2(\epsilon)}} d\epsilon = 0. \quad (64)$$

The integration over ϵ has been divided two intervals, namely (i) the vicinity of Fermi surface $\epsilon \in [-1, 1]$, where terms of both types indicated above will appear, and (ii) the tail $\epsilon \in [1, \infty]$, where a simple series in d_F^2 is generated,

$$\int_1^\infty \frac{\sqrt{\epsilon+1}\phi(\epsilon)\chi(\epsilon)d\epsilon}{2\sqrt{\epsilon^2 + d_F^2\chi^2(\epsilon)}} \simeq \int_1^\infty \frac{\sqrt{\epsilon+1}\phi(\epsilon)\chi(\epsilon)}{2|\epsilon|} d\epsilon - \frac{d_F^2}{2} \epsilon_F^2 \int_1^\infty \frac{\sqrt{\epsilon+1}\phi(\epsilon)\chi^3(\epsilon)}{2|\epsilon|^3} d\epsilon + \dots \quad (65)$$

Extracting the logarithmic contribution from the second term of equation (64), we have

$$\begin{aligned} \frac{2}{N(0)v_F} + \ln \frac{2}{d_F} + \ln \frac{1}{2} \left(1 + \sqrt{1 + d_F^2} \right) \\ + \frac{1}{2} \int_{-1}^1 \frac{\sqrt{\epsilon+1}\phi(\epsilon)\chi(\epsilon) - 1}{\sqrt{\epsilon^2 + d_F^2\chi(\epsilon)^2}} + \frac{1}{2} \int_1^\infty d\epsilon \frac{\sqrt{\epsilon+1}\phi(\epsilon)\chi(\epsilon)}{\sqrt{\epsilon^2 + d_F^2\chi(\epsilon)^2}} \end{aligned}$$

$$+ \frac{1}{2} \int_{-1}^1 d\epsilon \frac{\sqrt{\epsilon^2 + d_F^2} - \sqrt{\epsilon^2 + d_F^2} \chi^2(\epsilon)}{\sqrt{\epsilon^2 + d_F^2} \sqrt{\epsilon^2 + d_F^2} \chi^2(\epsilon)} = 0. \quad (66)$$

The leading approximation to d_F ,

$$d_F^0 = 2 \exp \left[\frac{2}{v_F N(0)} + \frac{1}{2} \int_{-1}^1 \frac{d\epsilon}{|\epsilon|} \left(\sqrt{\epsilon + 1} \phi(\epsilon) \chi(\epsilon) - 1 \right) + \frac{1}{2} \int_1^\infty \frac{d\epsilon}{\epsilon} \sqrt{\epsilon + 1} \phi(\epsilon) \chi(\epsilon) \right], \quad (67)$$

is obtained by setting $d_F \equiv 0$ everywhere except within the first logarithmic term of eq. (66). The first term inside the square brackets is the usual BCS contribution and is clearly dominant if the interaction is weak and localized in momentum space around the Fermi surface. If – as is the case for nuclear forces – the localization requirement is not fulfilled, the contribution from the second term of eq. (67) must also be taken into account. One can then derive meaningful results even for potentials with positive v_0 . The approximant (67) is offered as a useful generalization of the BCS weak-coupling formula to a broad class of pairing interactions.

The first correction and higher corrections to the formula (67) may be developed as follows. Near the Fermi surface, the denominators appearing in eq. (66) are simplified by noting that

$$\epsilon^2 + d_F^2 \chi^2(\epsilon) = \epsilon^2 + d_F^2 + d_F^2 [\chi^2(\epsilon) - 1] \quad (68)$$

can be expanded in powers of $d_F^2 [\chi^2(\epsilon) - 1] / (\epsilon^2 + d_F^2)$. This is a small quantity: for $\epsilon > d_F$ it is of order d_F^2 / ϵ^2 , while for $\epsilon < d_F$ we can make the expansion

$$\chi(\epsilon) = 1 + \chi'_0 \epsilon + \frac{1}{2} \chi''_0 \epsilon^2 + \dots, \quad (69)$$

where the subscript 0 stands for $\epsilon = 0$, and use

$$\frac{2\epsilon d_F}{\epsilon^2 + d_F^2} \leq 1. \quad (70)$$

(The prime indicates the derivative with respect to ϵ , while the subscript 0 stands for $\epsilon = 0$.) Accordingly, we invoke the expansion

$$\frac{1}{\sqrt{\epsilon^2 + d_F^2} \chi^2} = \frac{1}{\sqrt{\epsilon^2 + d_F^2}} \left[1 - \frac{1}{2} d_F^2 \frac{\chi^2 - 1}{\epsilon^2 + d_F^2} + \frac{3}{8} d_F^4 \frac{(\chi^2 - 1)^2}{(\epsilon^2 + d_F^2)^2} - \dots \right]. \quad (71)$$

At this point, any smooth functions in the numerators of the integral terms in eq. (66) may be expanded in Taylor series. Since (i) the integrations in the

fourth and sixth addends on the l.h.s. of (66) are performed on a symmetric interval and (ii) the denominators contain only even powers of ϵ , we need only consider terms with even powers of ϵ in the corresponding numerators. For example,

$$\int_{-1}^1 d\epsilon \frac{\sqrt{\epsilon^2 + d_F^2} - \sqrt{\epsilon^2 + d_F^2 \chi^2(\epsilon)}}{\sqrt{\epsilon^2 + d_F^2} \sqrt{\epsilon^2 + d_F^2 \chi^2(\epsilon)}} = \quad (72)$$

$$\begin{aligned} & -\frac{1}{2} d_F^2 \int_{-1}^1 d\epsilon \frac{\chi^2 - 1}{(\epsilon^2 + d_F^2)^{\frac{3}{2}}} + \frac{3}{8} d_F^4 \int_{-1}^1 d\epsilon \frac{(\chi^2 - 1)^2}{(\epsilon^2 + d_F^2)^{\frac{5}{2}}} - \dots \\ & = -\frac{1}{2} d_F^2 [(\chi'_0)^2 + \chi''_0] \left[-2 + 2 \ln \frac{2}{d_F} \right] + \frac{3}{8} d_F^4 4(\chi'_0)^2 \left[\frac{2}{3} \frac{1}{d_F^2} - 1 \right] \dots \end{aligned}$$

This step reveals a slight complication in the analysis. The integral of the first term of the Taylor expansion of $\chi^2 - 1$ vanishes, and consequently the integral of the second term of this Taylor expansion is of the same order as the integral of the term of the expansion (71) containing $(\chi^2 - 1)^2$ are of the same order in d_F .

In evaluating corrections to the result (67), it is convenient to define

$$I_n^m \equiv \int_{-1}^1 d\epsilon \frac{\epsilon^{2n}}{(\epsilon^2 + d_F^2)^{m+\frac{1}{2}}} \quad (73)$$

and

$$A_n \equiv (\sqrt{\epsilon + 1} \phi \chi^n)''_0. \quad (74)$$

The first correction to d_F^0 is then determined by applying recursion relations involving the I_n^m (see ref. [117]). Eq. (64) is written as

$$0 \simeq -\ln \frac{2}{d_F^0} + \frac{1}{4} d_F^2 B + \left(1 - \frac{1}{4} d_F^2 A_3 \right) \ln \frac{2}{d_F}, \quad (75)$$

where

$$B = -\int_1^\infty \frac{\sqrt{\epsilon + 1}}{\epsilon^3} \phi(\epsilon) \chi^3(\epsilon) d\epsilon - \int_{-1}^1 \frac{1}{|\epsilon|^3} \left[\sqrt{\epsilon + 1} \phi \chi^3 - 1 - \frac{1}{2} \epsilon^2 A_3 \right] d\epsilon$$

$$-\frac{1}{4}A_1 + \frac{1}{2}A_3 + \frac{1}{4}A_5 + 1, \quad (76)$$

and the improved estimate is

$$d_F \simeq d_F^0 \left[1 + \frac{1}{4} (d_F^0)^2 \left(B - A_3 \ln \frac{2}{d_F^0} \right) \right] \quad (77)$$

follows.

A calculation for the Argonne v_{14} interaction illustrates the utility and accuracy of the leading approximation (67) to the energy gap $\Delta_F = \epsilon_F d_F$ within the small-parameter expansion. In fig. (9), the k_F dependence of Δ_F as given by the zeroth-order approximation in d_F is compared with the essentially exact result obtained by iteration of eqs. (60) and (61). Free single-particle energies ($m^* = 1$) are assumed. The estimate (67) produces excellent results, especially at densities beyond the peak of the Δ_F curve.

The same strategy of constructing approximants to the gap problem through small-parameter expansion is applicable to pairing in higher angular momentum states and in particular to 3P_2 pairing. By way of illustration, consider the Type 1 ($M = \pm 2$) solution of the uncoupled-channel problem. The transformed gap equation (28) associated with this case has a form similar to that for 1S_0 pairing, with differences arising from the anisotropy of the P-wave problem. A weight factor $3(\sin^2 \theta)/2 = 3(1 - \cos^2 \theta)/2$ appears in the integration over angles in eq. (28), and $3\Delta_F^2(1 - \cos^2 \theta)/2$ appears in place of Δ_F^2 inside the square-root energy denominator. Doing the k integral first, we can directly exploit results and relations of sects. 4 and 5 (specifically, the first of eqs. (25) along with eqs. (26) and (36)). Ignoring corrections proportional to $d_F^2 = \Delta_F/\epsilon_F$, the only additional term that needs to be considered, relative to the angle-average approximation, is

$$\int d\mathbf{n} \frac{3}{2}(1 - \cos^2 \theta) / \ln \left[\frac{3}{2}(1 - \cos^2 \theta) \right]. \quad (78)$$

For the Type 2 solution (with $M = 0$), the additional term has the slightly different expression (see the last of eqs.(25))

$$\int d\mathbf{n} \frac{1}{2}(1 + 3 \cos^2 \theta) / \ln \left[\frac{1}{2}(1 + 3 \cos^2 \theta) \right]. \quad (79)$$

The most salient points are that both these contributions are of order unity relative to the dominant logarithm in the gap and both are negative. We may thus conclude that the true gap will be smaller than that given by the angle-average approximation and that the correction to the gap value calculated in this approximation will generally be small.

References

- [1] A. B. Migdal, Sov. Phys. JETP **10** (1960) 176
- [2] L. N. Cooper, R. L. Mills and A. M. Sessler, Phys. Rev. **114** (1959) 1377
- [3] R. L. Mills, A. M. Sessler, S. A. Moszkowski, and D. G. Shankland, Phys. Rev. Lett. **3** (1959) 381
- [4] V. J. Emery, Nucl. Phys. **12** (1959) 69; **19** (1960) 154
- [5] K. Nakamura, Progr. Theor. Phys. **21** (1959) 713; **24** (1960) 1195
- [6] K. A. Brueckner, T. Soda, P. W. Anderson, and P. Morel, Phys. Rev. **118** (1960) 1442
- [7] V. J. Emery and A. M. Sessler, Phys. Rev. **119** (1960) 248
- [8] T. Marumori, T. Murota, S. Takagi, and M. Yasuno, Prog. Theor. Phys. **25** (1961) 1035
- [9] T. Ishihara, R. Tamagaki, H. Tanaka, and M. Yasuno, Progr. Theor. Phys. **30** (1963) 601
- [10] E. M. Henley and L. Wilets, Phys. Rev. **133** (1964) B1118
- [11] R. Kennedy, L. Wilets, and E.M. Henley, Phys. Rev. **133** (1964) B1131
- [12] V. Ginzburg, Sov. Phys. JETP **20** (1965) 1346
- [13] H. Bando and S. Nagata, Prog. Theor. Phys. **35** (1966) 1026
- [14] E. Jakeman and S. A. Moszkowski, Phys. Rev. **141** (1966) 933
- [15] R. C. Kennedy, Nucl. Phys. **A118** (1968) 189
- [16] G. Baym, C. Pethick, and D. Pines, Nature **224** (1969) 673
- [17] V. Ginzburg, J. Stat. Phys. **1** (1969) 3
- [18] J. W. Clark and N.-C. Chao, Lett. Nuovo Cimento **2** (1969) 185
- [19] N. Itoh, Prog. Theor. Phys. **42** (1969) 1478
- [20] J. W. Clark and C. H. Yang, Lett. Nuovo Cimento **3** (1970) 272; **2** (1971) 379
- [21] S. Ikeuchi, S. Nagata, T. Mizutani, and K. Nakazawa, Prog. Theor. Phys. **46** (1971) 95
- [22] M. Hoffberg, A. E. Glassgold, R. W. Richardson, and M. Ruderman, Phys. Rev. Lett. **24** (1970) 775
- [23] R. Tamagaki, Progr. Theor. Phys. **44** (1970) 905
- [24] T. Takatsuka and R. Tamagaki, Progr. Theor. Phys. **46** (1971) 114

- [25] C.-H. Yang, J.W. Clark, Nucl. Phys. **A174** (1971) 49
- [26] N.-C. Chao, J. W. Clark, and C.-H. Yang, Nucl. Phys. **179** (1972) 320
- [27] C.-H. Yang and J. W. Clark, Lett. Nuovo Cimento **4** (1972) 969
- [28] E. Krotscheck, Z. Phys. **251** (1972) 135
- [29] T. Takatsuka, Progr. Theor. Phys. **47** (1972) 1062
- [30] T. Takatsuka, Progr. Theor. Phys. **48** (1972) 1517
- [31] T. Takatsuka, Progr. Theor. Phys. **50** (1973) 1754, 1755
- [32] J.W. Clark, C.-G. Källman, C.-H. Yang, and D. Chakkalakal, Phys. Lett. **B61** (1976) 331
- [33] R. Tamagaki, T. Takatsuka, and H. Fukawa, Prog. Theor. Phys. **64** (1980) 2107
- [34] E. Krotscheck and J. W. Clark, Nucl. Phys. **A333** (1980) 77
- [35] E. Krotscheck, R. A. Smith, and A. D. Jackson, Phys. Rev. **B24** (1981) 6404
- [36] S. Fantoni, Nucl. Phys. **A363** (1981) 381
- [37] T. Takatsuka and R. Tamagaki, Progr. Theor. Phys. **65** (1981) 1333
- [38] T. Takatsuka, Progr. Theor. Phys. **71** (1984) 1432
- [39] L. Amundsen and E. Østgaard, Nucl. Phys. **A437** (1985) 487
- [40] L. Amundsen and E. Østgaard, Nucl. Phys. **A442** (1985) 163
- [41] J. M. C. Chen, J. W. Clark, E. Krotscheck, and R. A. Smith, Nucl. Phys. **A451** (1986) 509
- [42] W. H. Dickhoff, Phys. Lett. **B210** (1988) 15
- [43] M. F. Jiang and T. T. S. Kuo, Nucl. Phys. **A481** (1988) 294
- [44] T. Takatsuka and R. Tamagaki, Nucl. Phys. **A478** (1988) 785c
- [45] H. Kucharek, P. Ring, and P. Schuck, Z. Phys. **A334** (1989) 119
- [46] H. Kucharek, P. Ring., P. Schuck, R. Bengtsson, and M. Girod, Phys. Lett. **B216** (1989) 249
- [47] T. L. Ainsworth, J. Wambach, and D. Pines, Phys. Lett. **B222** (1989) 173
- [48] M. Baldo, J. Cugnon, A. Lejeune, and U. Lombardo, Nucl. Phys. **515** (1990) 409
- [49] T. Alm, G. Ropke, and M. Schmidt, Z. Phys. **A337** (1990) 355
- [50] W. H. Dickhoff, C. C. Gearhart, B. E. Vonderfecht, A. Polls, and A. Ramos, in Recent progress in many-body theories, vol. 2, ed. Y. Avishai (Plenum, New York, 1990), p. 141

- [51] B.E. Vonderfecht, C.C. Gearhart, W.H. Dickhoff, A. Polls, and A. Ramos, Phys. Lett. **B253** (1991) 1
- [52] M. Baldo, I. Bombaci, and U. Lombardo, Phys. Lett. **B283** (1992) 8
- [53] M. Baldo, J. Cugnon, A. Lejeune, and U. Lombardo, Nucl. Phys. **A536** (1992) 349
- [54] T. Alm, B. L. Friman, G. Röpke, and H. Schulz, Nucl. Phys. **A551** (1993) 45
- [55] J. M. C. Chen, J. W. Clark, R. D. Davé, and V.V. Khodel, Nucl. Phys. **A555** (1993) 59
- [56] J. Wambach, T. L. Ainsworth, and D. Pines, Nucl. Phys. **A555** (1993) 128
- [57] T. Takatsuka and R. Tamagaki, Progr. Theor. Phys. Suppl. **112** (1993) 27
- [58] S. Takahara, N. Onishi, and N. Tajima, Phys. Lett. **B331** (1994) 261
- [59] R. A. Broglia, F. De Blasio, G. Lazzari, M. Lazzari, and P. M. Pizzochero, Phys. Rev. **D50** (1994) 4781
- [60] M. Baldo, U. Lombardo, E. E. Saperstein, M. V. Zverev, Phys. Lett. **B350** (1995) 135
- [61] M. Baldo, U. Lombardo, and P. Schuck, Phys. Rev. **C52** (1995) 975
- [62] T. Takatsuka and R. Tamagaki, Prog. Theor. Phys. **94** (1995) 457
- [63] T. Alm, G. Röpke, A. Sedrakian, and F. Weber, Nucl. Phys. **A604** (1996) 491
- [64] F. De Blasio, G. Lazzari, P. M. Pizzochero, and R. A. Broglia, Phys. Rev. **D53** (1996) 4226
- [65] Ø. Elgarøy, L. Engvik, E. Osnes, F. V. De Blasio, M. Hjorth-Jensen, and G. Lazzari, Phys. Rev. **D54** (1996) 1848
- [66] H.-J. Schulze, J. Cugnon, A. Lejeune, M. Baldo, and U. Lombardo, Phys. Lett. **B375** (1996) 1
- [67] V. A. Khodel, V. V. Khodel, and J. W. Clark, Nucl. Phys. **A598** (1996) 390
- [68] Ø. Elgarøy, L. Engvik, M. Hjorth-Jensen, E. Osnes, Nucl. Phys. **A604** (1996) 466
- [69] Ø. Elgarøy, L. Engvik, M. Hjorth-Jensen, E. Osnes, Nucl. Phys. **A607** (1996) 425
- [70] Ø. Elgarøy, L. Engvik, M. Hjorth-Jensen, E. Osnes, Phys. Rev. Lett. **77** (1996) 1428
- [71] A. Sedrakian, T. Alm, and U. Lombardo, Phys. Rev. **C55** (1997) R582
- [72] B. V. Carlson, T. Frederico, and F. B. Guimarães, Phys. Rev. **C56** (1997) 3097

- [73] V.A. Khodel, *Yad. Fiz.* **60** (1997) 1157
- [74] T. Takatsuka and R. Tamagaki, *Prog. Theor. Phys.* **97** (1997) 263
- [75] V. A. Khodel, V. V. Khodel, and J. W. Clark, *Phys. Rev. Lett.* **81** (1998) 3828
- [76] F. V. De Blasio and G. Lazzari, *Mod. Phys. Lett.* **A13** (1998) 1383
- [77] Ø. Elgarøy, L. Engvik, M. Hjorth-Jensen, and E. Osnes, *Phys. Rev.* **C57** (1998) R1069
- [78] Ø. Elgarøy and M. Hjorth-Jensen, *Phys. Rev.* **C57** (1998) 1174
- [79] M. Baldo, Ø. Elgarøy, L. Engvik, M. Hjorth-Jensen, and H.-J. Schulze, *Phys. Rev.* **C58** (1998) 1921
- [80] J. W. Clark, V. A. Khodel, and V. V. Khodel, in *Condensed Matter Theories*, Vol. 13, eds. J. da Providencia and F. B. Malik (Nova Science Publishers, Commack, NY, 1998), p. 363
- [81] J. W. Clark, V. A. Khodel, and V. V. Khodel, in *Condensed Matter Theories*, Vol. 14, eds. D. Ernst et al. (Nova Science Publishers, Commack, NY, 1999), in press
- [82] T. Papenbrock and G. F. Bertsch, *Phys. Rev.* **C59** (1999) 2052
- [83] A. Hewish, S. J. Bell, J. D. .H. Pilkington, P. F. Scott, and R. A. Collins, *Nature* **217** (1968) 709
- [84] T. Gold, *Nature* **218** (1969) 731; **221** (1969) 25
- [85] O. Maxwell, *Ap. J.* **231** (1979) 201
- [86] B. Friman and O. V. Maxwell, *Ap. J.* **232** (1979) 541
- [87] S. Tsuruta, *Phys. Rep.* **56** (1979) 237
- [88] K. Nomoto and S. Tsuruta, *Ap. J.* **250** (1981) L19
- [89] K. Nomoto and S. Tsuruta, *Ap. J.* **312** (1987) 711
- [90] J. M. Lattimer, C. J. Pethick, M. Prakash, and P. Haensel, *Phys. Rev. Lett.* **66** (1991) 2701
- [91] C. J. Pethick, *Rev. Mod. Phys.* **64** (1992) 1133
- [92] M. Prakash, *Phys. Rep.* **242** (1994) 387
- [93] T. Takatsuka and R. Tamagaki, *Prog. Theor. Phys.* **97** (1997) 345
- [94] Ø. Elgarøy, L. Engvik, and E. Osnes, *Phys. Rev. Lett.* **76** (1996) 1994
- [95] Ch. Schaab, D. Voskresensky, et. al., *Astron. Astrophys.* **321** (1997) 591
- [96] G. Baym, C. Pethick, D. Pines, and M. Ruderman, *Nature* **224** (1969) 872
- [97] D. Pines and M. A. Alpar, *Nature* **316** (1985) 27

- [98] F. K. Lamb, in *Frontiers of stellar evolution*, ed. D. L. Lambert (Astronomy Society of the Pacific, San Francisco, 1991), p. 299
- [99] A. Alpar, Ü. Kiziloglŭ, and J. van Paradijs (eds.), *Lives of the neutron stars* (Kluwer, Dordrecht, 1995)
- [100] K. Riisager, *Rev. Mod. Phys.* **66** (1994) 1105
- [101] A. C. Mueller and B. M. Sherril, *Ann. Rev. Nuc. Part. Phys.* **43** (1993) 529
- [102] G. Baym and C. J. Pethick, *Ann. Rev. Nucl. Sci.* **25** (1975) 27;
G. Baym and C. J. Pethick, *Ann. Rev. Astron. Astrophys.* **17** (1979) 415;
C. J. Pethick and D. G. Ravenhall, *Ann. Rev. Nucl. Part. Phys.* **45** (1995) 429
- [103] S. L. Shapiro and S. A. Teukolsky, *Black holes, white dwarfs, and neutron stars: the physics of compact objects* (Wiley, New York, 1983)
- [104] R. B. Wiringa, V. Fiks, A. Fabrocini, *Phys. Rev.* **C38** (1988) 1010
- [105] J. Bardeen, L. N. Cooper, and J. R. Schrieffer, *Phys. Rev.* **108** (1957) 1175
- [106] J. R. Schrieffer, *Theory of superconductivity* (W. A. Benjamin, New York, 1964)
- [107] R. B. Wiringa, V. G. J. Stoks, and R. Schiavilla, *Phys. Rev.* **C51** (1995) 38
- [108] V. G. J. Stoks, R. A. M. Klomp, M. C. M. Rentmeester, and J. J. de Swart, *Phys. Rev.* **C48** (1993) 792
- [109] D. Vollhardt and P. Wölfle, *The superfluid phases of helium 3* (Taylor Francis, London, 1990)
- [110] R. Tamagaki, *Progr. Theor. Phys.* **39** (1968) 91
- [111] R. B. Wiringa, R. A. Smith, and T. L. Ainsworth, *Phys. Rev.* **C29** (1984) 1207
- [112] R. Machleidt, K. Holinde, and Ch. Elster, *Phys. Rep.* **149** (1987) 1
- [113] R. Machleidt, *Adv. Nucl. Phys.* **19** (1989) 189
- [114] R. Machleidt, F. Sammarruca, and Y. Song, *Phys. Rev.* **C53** (1996) R1483
- [115] V. G. J. Stoks, R. A. M. Klomp, C. P. F. Terheggen, and J.J. de Swart, *Phys. Rev.* **C49** (1994) 2950
- [116] M. Lacombe, B. Loiseau, J.-M. Richard, R. Vinh Mau, J. Côté, P. Pirès, and R. de Tournel, *Phys. Rev.* **C21** (1980) 861
- [117] V. V. Khodel, Ph.D. thesis (Washington University, St. Louis, 1997)
- [118] A. Migdal, *Rev. Mod. Phys.* **50** (1978) 107
- [119] A. B. Migdal, E. E. Saperstein, M. A. Troitsky, and D. N. Voskresensky, *Phys. Rep.* **192** (1990) 179

- [120] A. Akmal, V. R. Pandharipande, and D. G. Ravenhall, Phys. Rev. **C58** (1998) 1804
- [121] A. M. Dyugaev, Sov. Phys. JETP **43** (1976) 1247
- [122] A. M. Dyugaev, Sov. J. Nucl. Phys. **38** (1983) 680
- [123] E. Krotscheck, J. W. Clark, and A. D. Jackson, Phys. Rev. **B28** (1983) 5088
- [124] R. F. Bishop, Theor. Chim. Acta **80** (1991) 95

Table 1

Energy gap Δ_F for 3P_2 - 3F_2 pairing in neutron matter at several values of the Fermi momentum, for the Argonne v_{18} and v_{14} interactions and the OPEG potential. Free single-particle energies ($m^* = 1$) are used, except for the last column, where $m^* = 0.78$.

k_F	OPEG	v_{14}	v_{18}	$v_{18}(0.78)$
1.0	0.0009	0.0020	0.0020	—
1.5	0.1369	0.2496	0.1576	0.0263
2.0	0.5376	0.8028	0.4362	0.0947
2.2	0.6167	0.8519	0.4235	0.0875
2.3	0.6175	0.8182	0.3807	0.0740
2.5	0.5419	0.6542	0.2458	0.0384
3.0	0.1538	0.1330	0.0059	—

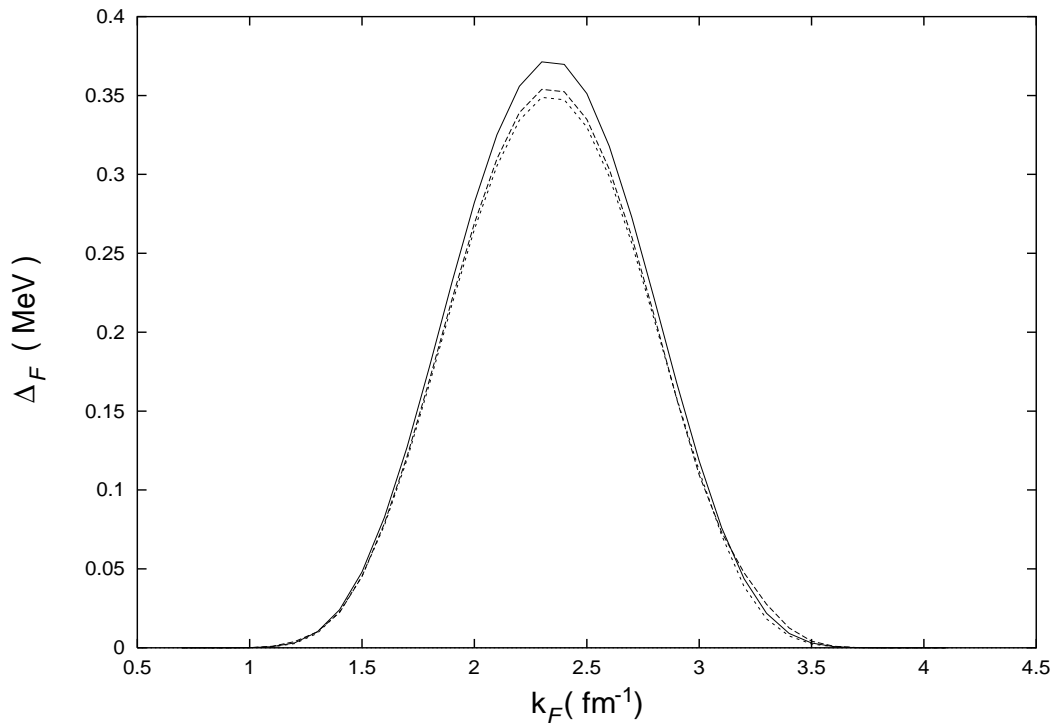


Fig. 1. Test of the angle-average approximation for 3P_2 pairing, without coupling to the 3F_2 state. The energy gap parameter Δ_F (square root of the quantity (7), evaluated at the Fermi surface) is plotted versus Fermi momentum k_F , for the pure $M = 0$ solution (long-dashed curve) and the $|M| = 2$ solution (short-dashed curve), and as calculated in the angle-average approximation (solid curve). The pairing matrix elements are constructed from the OPEG potential, and free single-particle energies are assumed ($m^* = 1$).

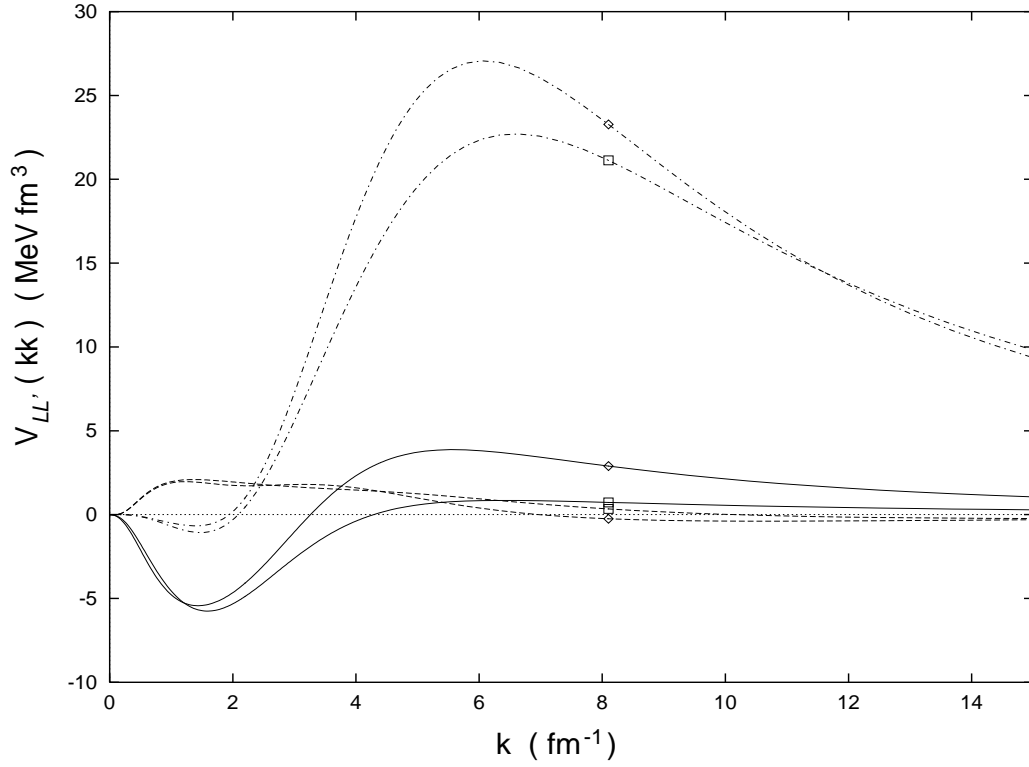


Fig. 2. Diagonal pairing matrix elements $V_{LL'}^{J=2}(k, k) = V_{11}(kk)$ (solid curves), $V_{13}(kk)$ (dashed curves), and $V_{33}(kk)$ (dot-dashed curves) in the 3P_2 - 3F_2 coupled channel, as functions of momentum k . Curves for the Argonne v_{14} and v_{18} interactions are labeled with a square and with a diamond, respectively.

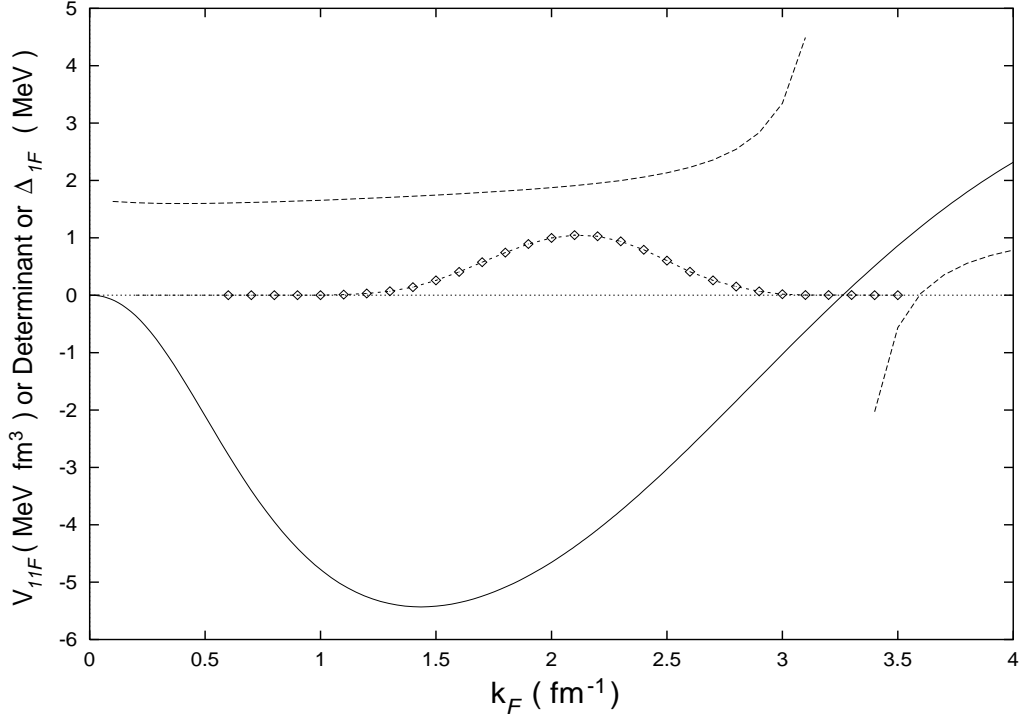


Fig. 3. Illustration of gap existence and closure for ${}^3\text{P}_2$ pairing by the Argonne v_{18} interaction, with coupling to the ${}^3\text{P}_2$ state turned off. Dependences on Fermi momentum k_F , of the diagonal matrix elements $V_{11}^{J=2}(k_F, k_F) \equiv V_{11F}$ of the pairing interaction (solid curve), the dimensionless characteristic determinant of the linearized version of system (20) (dashed curve), and the gap component value $\Delta_1^{2M}(k_F) \equiv \Delta_{1F}$ determined in angle-average approximation (dotted curve with diamonds). Free single-particle energies are assumed.

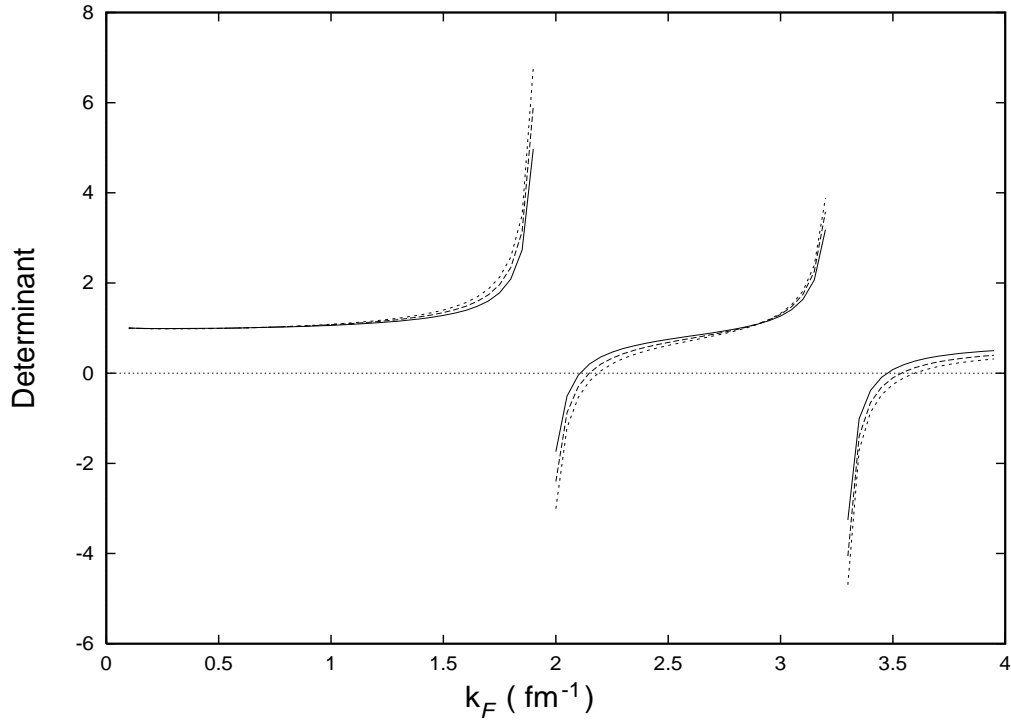


Fig. 4. The characteristic determinant for pairing in the 3P_2 - 3F_2 coupled channel as a function of Fermi momentum k_F . Results are shown for the Argonne v_{18} potential and three values of the parameter $m^* = M_n^*/M_n$ in an effective-mass approximation for the normal-state single-particle energies: $m^* = 1$ (short-dashed curve), $m^* = 0.8$ (long-dashed curve), and $m^* = 0.6$ (solid curve).

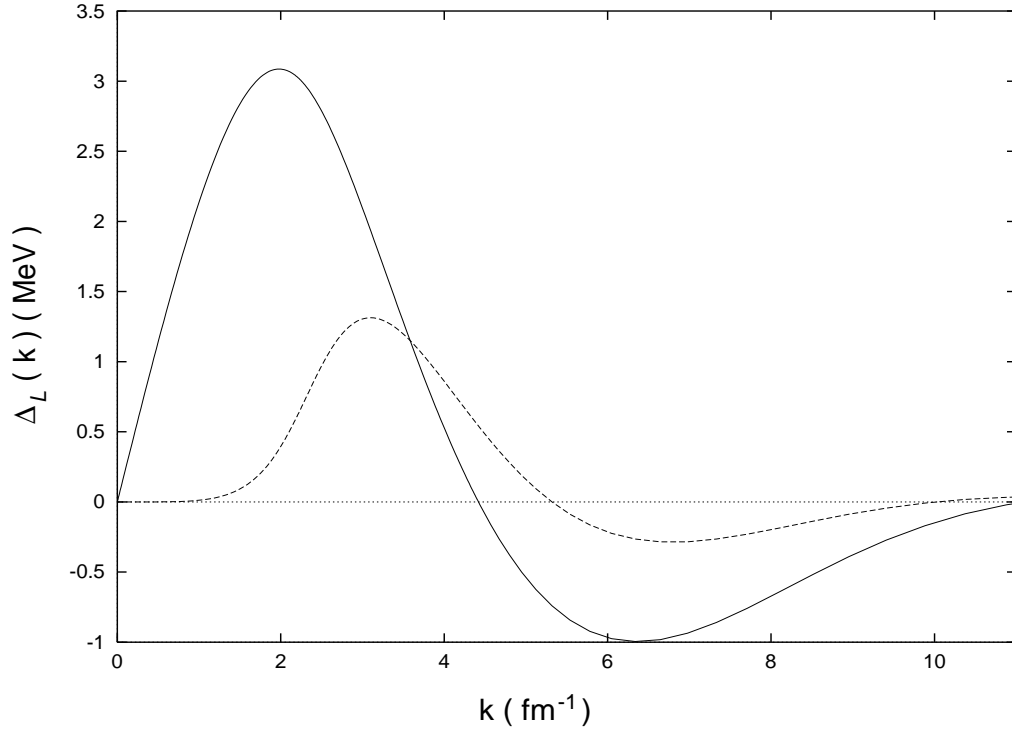


Fig. 5. Gap components $\Delta_1^{2M}(k) \equiv \Delta_1(k)$ (solid curve) and $\Delta_3^{2M}(k) \equiv \Delta_3(k)$ (dashed curve) for 3P_2 - 3F_2 pairing (coupled-channel case), calculated in angle-average approximation for the OPEG potential and $m^* = 1$, and plotted versus momentum k at $k_F = 2.2 \text{ fm}^{-1}$.

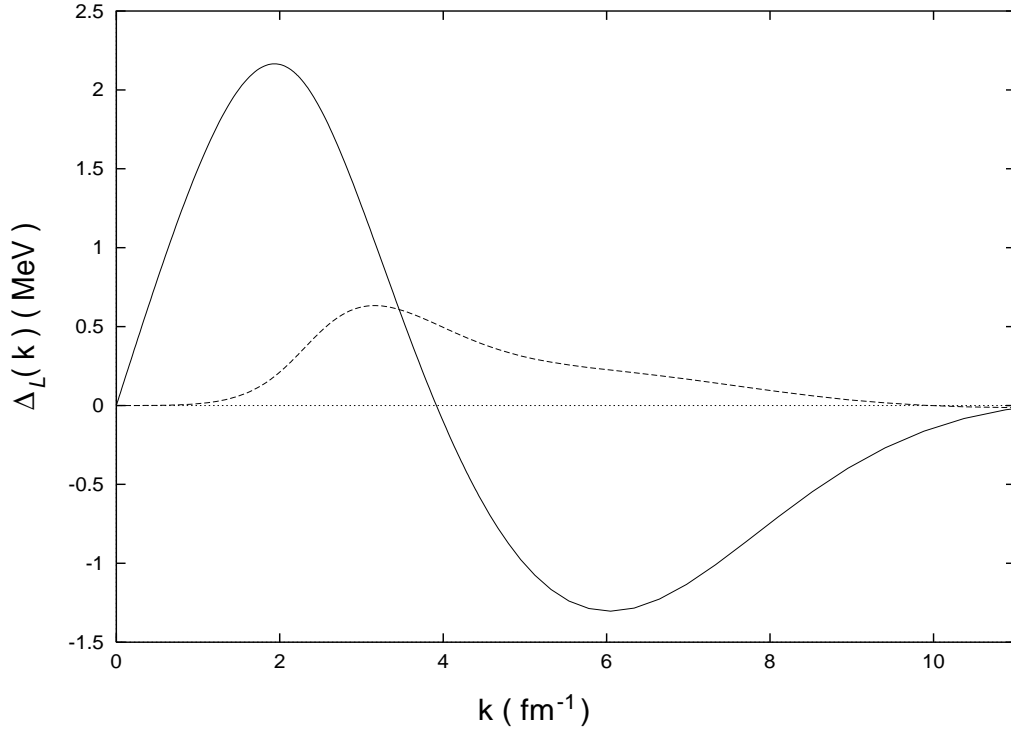


Fig. 6. Gap components $\Delta_1^{2M}(k) \equiv \Delta_1(k)$ (solid curve) and $\Delta_3^{2M}(k) \equiv \Delta_3(k)$ (dashed curve) for 3P_2 - 3F_2 pairing (coupled-channel case), calculated in angle-average approximation for the Argonne v_{18} potential and $m^* = 1$, and plotted versus momentum k at $k_F = 2.2 \text{ fm}^{-1}$.

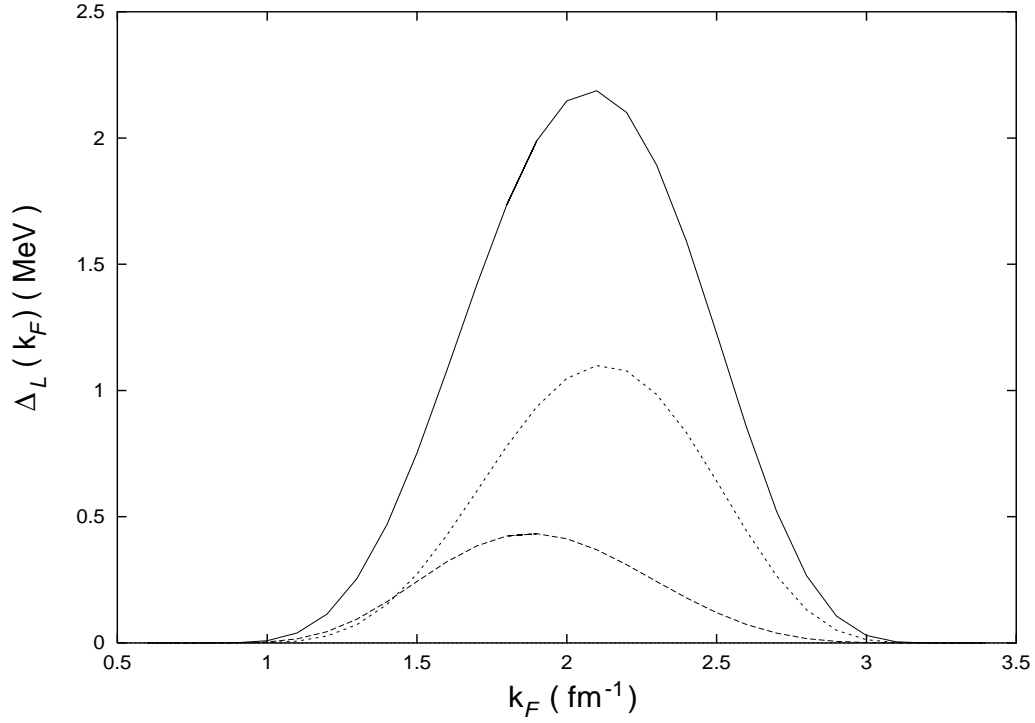


Fig. 7. Gap-component values $\Delta_1^{2M}(k_F) \equiv \Delta_1(k_F)$ (solid curve) and $\Delta_3^{2M}(k_F) \equiv \Delta_3(k_F)$ (long-dashed curve) *with* channel coupling, and $\Delta_1(k_F)$ *without* channel coupling (short-dashed curve), calculated in angle-average approximation for the Argonne v_{18} potential and $m^* = 1$, and plotted as a function of Fermi momentum k_F .

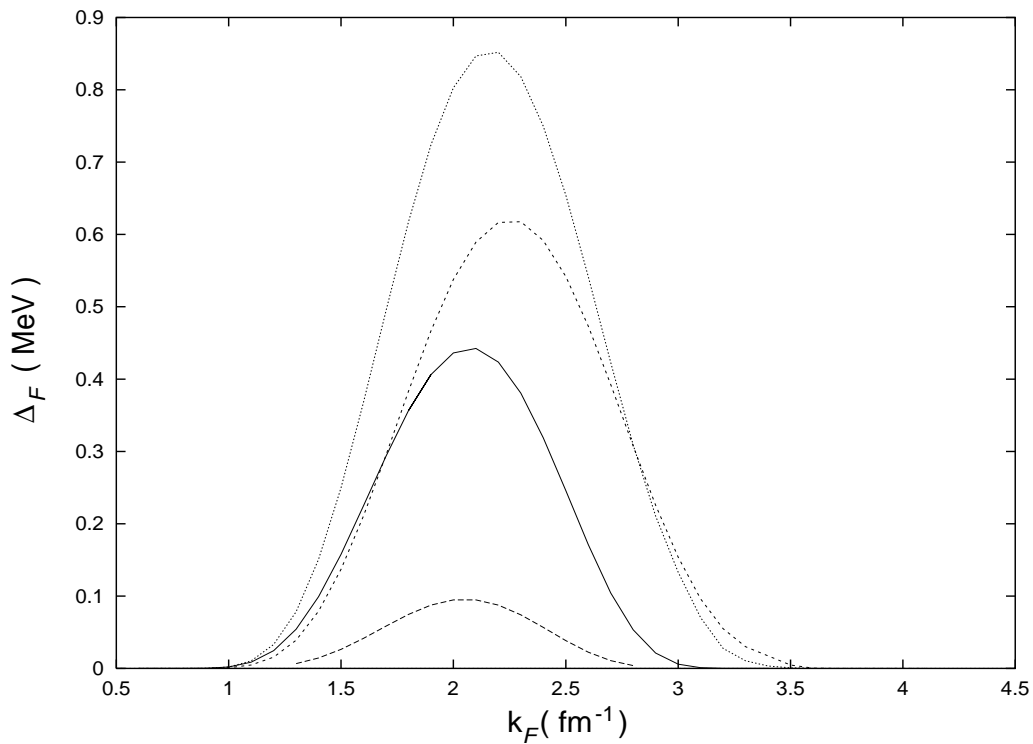


Fig. 8. Dependence on Fermi momentum k_F of the overall gap measure Δ_F (square root of the quantity (7), evaluated at the Fermi surface) for coupled-channel 3P_2 - 3F_2 neutron pairing, as determined in the angle-average approximation. Dotted curve: for Argonne v_{14} interaction and effective-mass parameter $m^* = 1$. Short-dashed curve: for OPEG potential and $m^* = 1$. Solid curve: for Argonne v_{18} potential and $m^* = 1$. Long-dashed curve: for Argonne v_{18} interaction and $m^* = 0.78$.

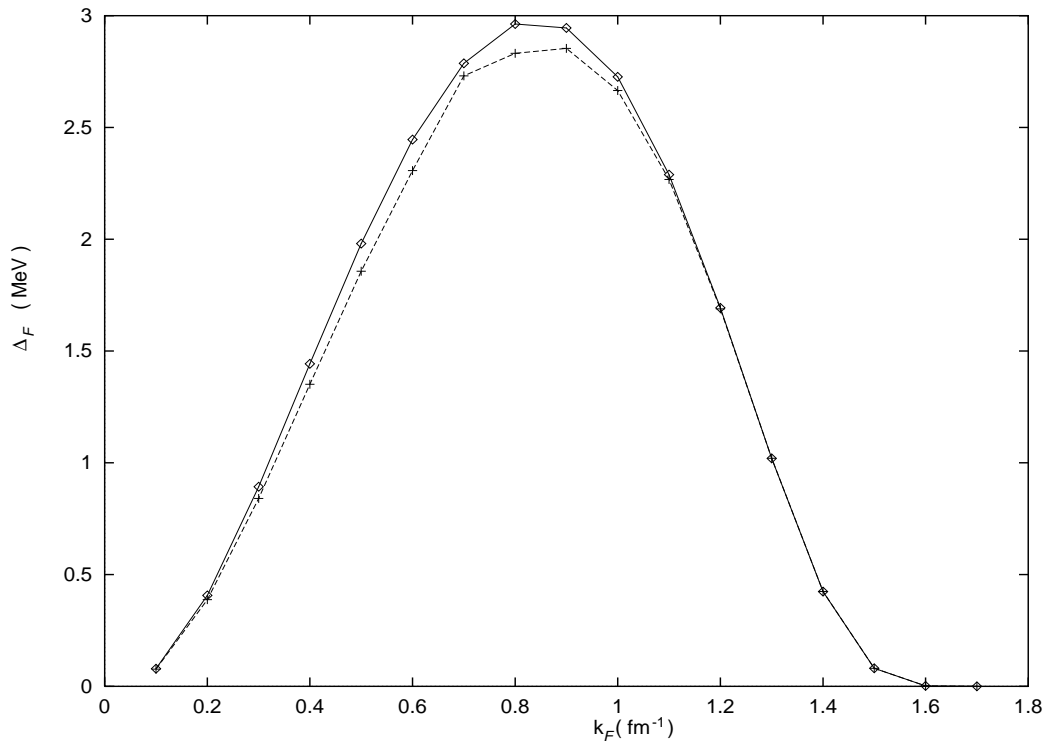


Fig. 9. Superfluid energy-gap amplitude Δ_F in the 1S_0 channel, plotted as a function of Fermi momentum k_F for the Argonne v_{18} potential and $m^* = 1$, as calculated “exactly” by iteration (solid curve) and to leading approximation in the smallness parameter d_F (dashed curve).